Virology 486 (2015) 158–172

Contents lists available at ScienceDirect

Virology

journal homepage: www.elsevier.com/locate/yviro

Mungbean yellow mosaic Indian virus encoded AC2 protein suppresses RNA silencing by inhibiting Arabidopsis RDR6 and AGO1 activities

Vikash Kumar [a,b,*,1], Sumona Karjee Mishra [a], Jamilur Rahman [a,c], Jyoti Taneja [a,d], Geethaa Sundaresan [a], Neeti Sanan Mishra [a], Sunil K. Mukherjee [a,e,*]

[a] Plant Molecular Biology, International Centre for Genetic Engineering and Biotechnology, Aruna Asaf Ali Marg, New Delhi 110067, India
[b] Department of Physiology, Medical College of Wisconsin, 8701 Watertown Plank Road, Milwaukee 53226, USA
[c] Department of Genetics & Plant Breeding, Sher-e-Bangla Agricultural University, Dhaka 1207, Bangladesh
[d] Department of Plant and Microbial Biology, University of California, Berkeley, CA 94720, USA
[e] Department of Genetics, University of Delhi, South Campus, Benito Juarez Marg, New Delhi 110021, India

ARTICLE INFO

Article history:
Received 28 January 2015
Returned to author for revisions
14 February 2015
Accepted 15 August 2015
Available online 1 October 2015

Keywords:
AC2
AGO1
Geminivirus
PTGS
RDR6
TasiRNA

ABSTRACT

RNA silencing refers to a conserved RNA-directed gene regulatory mechanism in a wide range of eukaryotes. It plays an important role in many processes including growth, development, genome stability, and antiviral defense in the plants. Geminivirus encoded AC2 is identified as an RNA silencing suppressor protein, however, the mechanism of action has not been characterized. In this paper, we elucidate another mechanism of AC2-mediated suppression activity of *Mungbean Yellow Mosaic India Virus* (MYMIV). The AC2 protein, unlike many other suppressors, does not bind to siRNA or dsRNA species and its suppression activity is mediated through interaction with key components of the RNA silencing pathway, *viz.,* RDR6 and AGO1. AC2 interaction inhibits the RDR6 activity, an essential component of siRNA and tasi-RNA biogenesis and AGO1, the major slicing factor of RISC. Thus the study identifies dual sites of MYMIV-AC2 interference and probably accounts for its strong RNA silencing suppression activity.

Introduction

RNA-mediated gene silencing is a highly conserved mechanism of sequence-dependent gene regulation involving suppression of transcription, transcript degradation or translation inhibition (Agarwal et al., 2003; Sanan-Mishra et al., 2009; Kumar et al., 2014). The process of RNA silencing has been detailed by studies in several model organisms, such as *Arabidopsis thaliana, Caenorhabditis elegans* and *Drosophila melanogaster*. The phenomenon has since been implicated in a variety of biological processes from organism development to host defense pathways. The trigger of RNA silencing is a double-stranded RNA (dsRNA) or an imperfectly self-folded hairpin RNA molecule, which is processed into 21–24 nucleotide short interfering RNA (siRNA) or microRNA (miRNA) duplex by the RNAse III-type enzyme, DICER. The small RNA duplex is then incorporated into a ribonucleoprotein complex called RNA-Induced Silencing Complex (RISC) that eventually cleaves/inhibits any mRNA complementary to the small RNA contained within it (Bartel, 2004; Tomari and Zamore, 2005). In plants a subset of RNA-dependent RNA polymerases (RDR) are involved in siRNA amplification process which ensures further persistence and systemic spread of RNA silencing, even in the absence of the immediate dsRNA trigger (Agarwal et al., 2003).

Viruses are both initiators and targets of gene silencing (Pruss et al., 1997; Rahman et al., 2012). Virus-induced gene silencing is elicited by dsRNA intermediates of replicating viruses, RDR1- or RDR6-mediated formation of dsRNAs or structured regions of viral RNAs (Voinnet, 2005; Pantaleo et al., 2007). The RNAi based antiviral defense mechanism is thus the major obstacle towards virus multiplication and pathogenicity. As a counter defensive strategy the viruses have successfully acquired RNA silencing suppressor (RSS) functions by which they are able to restrict the silencing machinery for efficient replication and systemic spread in the host. It is believed that these proteins have evolved independently in various viruses as they do not share any common

Abbreviations: MYMIV, *Mungbean Yellow Mosaic India Virus*; PTGS, post-transcriptional gene silencing; TGS, transcriptional gene silencing; RDR6, RNA dependent RNA polymerase; RISC, RNA-Induced Silencing Complex; RSS, RNA silencing suppressor; TrAP, Transcriptional Activator Protein; NLS, nuclear localization signal; EMSA, electrophoretic mobility shift assay; ToLCV, *Tomato leaf curl virus*

* Corresponding authors at: Plant Molecular Biology, International Centre for Genetic Engineering and Biotechnology, Aruna Asaf Ali Marg, New Delhi 110067, India.

E-mail addresses: vikashkumarhi@yahoo.com, vkumar@mcw.edu (V. Kumar), sunilmukherjee@hotmail.com (S.K. Mukherjee).

[1] Present address: Department of Physiology, Medical College of Wisconsin, 8701 watertown Plank Road, Milwaukee 53226, USA.

http://dx.doi.org/10.1016/j.virol.2015.08.015
0042-6822/

signature sequences and are structurally as well as functionally dissimilar from each other. The first clue about RSS came from observations on 'synergism' where disease severity from one virus was found to exacerbate in presence of co-infection by a second unrelated virus. This led to the discovery of potyviral Helper component proteinase (HcPro) as the synergism determinant in potex–potyvirus interaction. This was subsequently proved to be an RSS (Anandalakshmi et al., 1998; Kasschau and Carrington, 1998) and eventually many more RSS have been identified from both plant and animal viruses.

The mechanism of suppression for most RSS proteins is still elusive. The common strategy for suppression that has been identified for many such proteins includes long/short dsRNA binding activity (Lakatos et al., 2006; Pumplin and Voinnet, 2013). A few proteins harboring glycine-tryptophan repeats (GW) are also known to function as RSS (Giner et al., 2010). Moreover, there are RSS proteins which have been found to interact with other proteins of the silencing pathway, such as, cucumovirus encoded 2b that binds to AGO1 and inhibits its enzymatic activity (Zhang et al., 2006) while polerovirus-encoded P0 targets the PAZ motif of AGO1 and FHV-B2 inhibits PAZ motif of DCL1 (Baumberger et al., 2007; Bortolamiol et al., 2008; Singh et al., 2009).

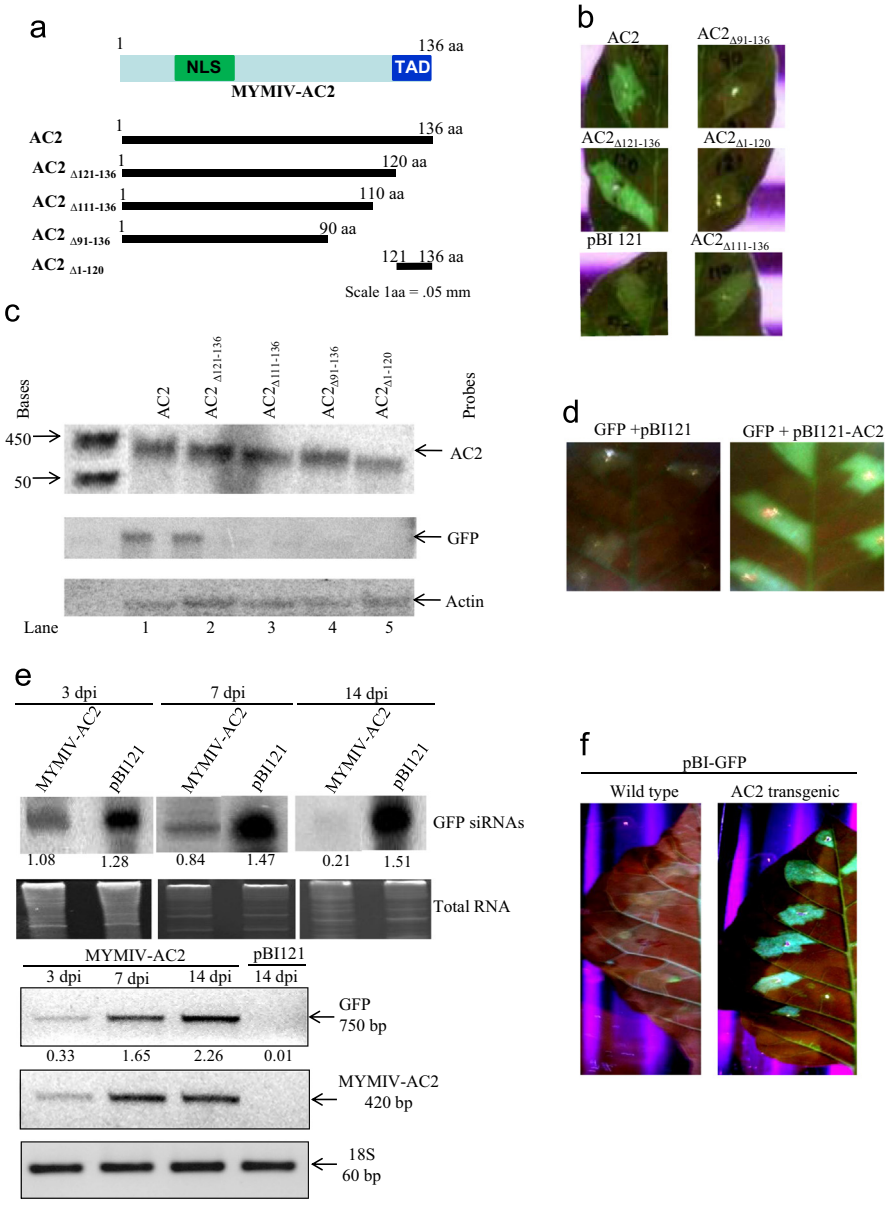

Fig. 1. MYMIV-AC2 acts as an RNA silencing suppressor and interferes with the accumulation of siRNA (a) Schematic representation showing the various domains of full length MYMIV-AC2 construct and the various deletion mutations generated for the study. (b) Leaves of GFP silenced tobacco plants were infiltrated with empty vector, AC2, $AC2_{\Delta 121-136}$, $AC2_{\Delta 111-136}$, $AC2_{\Delta 91-136}$ or $AC2_{\Delta 1-120}$ as indicated at the top of each photograph. Reversion of GFP Silencing in infiltrated areas was analyzed at 7 dpi under UV light as shown in the photographs. (c) mRNA levels of full length AC2 or its deletions (upper panel) and GFP (middle panel) were analyzed by northern blots. Actin (bottom panel) was used as an internal loading control. (d) Leaves of wild type *N. benthamiana* were co-infiltrated with mixture of agrobacteria containing the binary vectors encoding AC2 or empty vector along with GFP expressing constructs as indicated. GFP fluorescence was visualized 6dpi under UV light. (e) GFP silenced line were agroinfilterated with empty vector or AC2 expressing constructs. Total RNA was extracted from the unifiltrated and agroinfiltrated areas 3 dpi, 6 dpi, and 14 dpi and separated on 15% denaturing polyacrylamide to analyze the level of GFP siRNAs. The value under each lane of blot represents the ratio of siRNA intensities with respect to the total RNA. The expression of GFP and AC2 proteins was validated by semi-quantitative RT-PCR. The degree of GFP reversal by AC2 is shown below the gel. 18S rRNA was used as an internal control. (f) Leaves of wild type and AC2 transgenic of *N. benthmiana* were agroinfiltrated with GFP expressing constructs. GFP fluorescence was visualized 6 dpi under UV light.

The geminiviruses constitute the second largest family of plant viruses and have a very long recorded history for pathogenicity. They are capable of infecting almost all types of plant species with few exceptions and are associated with some of the most devastating plant diseases like leaf curls in cotton, pepper and tomatoes, mosaic and yellow mosaic of cassava, pulses and beans. Of the seven different genera of the geminiviruses, begomoviruses constitute the largest one (Adams et al., 2013). The begomovirus-encoded AC2 protein is generally a strong pathogenicity factor (Voinnet et al., 1999). It is a ~15 kDa protein and is required for the transcriptional activation of late viral genes, namely the pre-coat and coat-proteins, and thus is also known as Transcriptional Activator Protein (TrAP) (Sunter and Bisaro, 1991a, 1991b; Jeffrey et al., 1996; Trinks et al., 2005). In general, the AC2 protein has a modular structure consisting of three conserved domains: a basic domain with a nuclear localization signal (NLS) at the N-terminus, a central DNA-binding Zn-finger motif ($C_{37}X_1C_{39}X_7C_{47}X_6H_{54}X_4H_{59}C_{60}$) and a C-terminal acidic transactivation domain (Hartitz et al., 1999). It binds to ssDNA in a non-specific way and binds only weakly to dsDNA, suggesting that it is not a canonical transcriptional factor, but probably interacts with host plant cellular proteins to trigger transcriptional activation (Hartitz et al., 1999). Furthermore, AC2 interacts and inactivates SNF1 and adenosine kinases, enzymes which appear to be involved in defense response (Hao et al., 2003; Wang et al., 2003). It thus alters the activities of several cellular proteins or protein complexes to control the host machinery for disease establishment.

In addition, AC2 proteins have been shown to have multiple RNA silencing suppressor mechanisms. Some of them required transactivational potential whereas some of them do not require transcription activation (Van et al., 2002; Dong et al., 2003; Trinks et al., 2005; Bisaro 2006). AC2 proteins can suppress both post transcriptional gene silencing (PTGS) and transcriptional gene silencing (TGS) (Buchmann et al., 2009; Raja et al., 2010). Though suppression of TGS by AC2 proteins has been well studied, the true mechanism of AC2-mediated suppression of PTGS is relatively unknown. Previously, we reported that AC2 protein of *Mung bean yellow mosaic India virus* (MYMIV-AC2) is a potent RSS (Karjee et al., 2008). Here we attempt to understand the molecular principles behind the RSS function of MYMIV-AC2. We show that AC2 interacts with RDR6 and AGO1 to suppress siRNA biogenesis and abrogate the RISC activity, respectively.

Results

MYMIV-AC2 acts as an RNA silencing suppressor and interferes with the accumulation of siRNA

Previously, we have shown that MYMIV-AC2 is a silencing suppressor using the GFP silenced *Nicotiana Xanthi* plants (Rahman et al., 2012; Karjee et al., 2008). Next, we wanted to study the domain responsible for silencing suppression. In order to investigate this we made series of deletion mutants (Fig. 1a). The leaves of GFP silenced *N. tabaccum cv. xanthi* line were agro-infiltrated separately with full length and deletion mutants of MYMIV-AC2 each expressing under the control of CaMV35S promoter. The C-terminal deletion mutant $AC2_{\Delta 121-136}$ showed GFP reversion equivalent to the full length AC2 (Fig. 1b). However, all the other deletion mutants showed negative response in this assay (Fig. 1b). The results were further confirmed with the molecular analysis for GFP mRNA levels (Fig. 1c). Northern analysis showed that GFP mRNA was abundant in the bright green fluorescent patches infiltrated with 35S-AC2 or 35S-$AC2_{\Delta 121-136}$ (Fig. 1c lanes 1–2). No GFP specific mRNA band was observed in the lanes corresponding to 35S-$AC2_{\Delta 1-120}$, 35S-$AC2_{\Delta 91-136}$ and 35S-$AC2_{\Delta 111-136}$, similar to the empty vector infiltrated zones (Fig. 1c lanes 3–5). It is noteworthy that all the deletion mutants of AC2 expressed transcripts in the infiltrated zone to the similar extent. Taken together, it suggested that the domain comprising the first 120 residues of the MYMIV-AC2 protein governs its suppression activity.

To investigate the mechanism of MYMIV-AC2 RSS activity, its effect on siRNA levels were analyzed. 35S-GFP and 35S-AC2 constructs were co-infiltrated in wild type tobacco leaves and the kinetics of GFP fluorescence was compared with the control sample in which GFP was co-infiltrated with the empty vector. In the control set 35S-GFP ceased to fluoresce 6 dpi due to induction of sense gene-mediated silencing. However, co-infiltration with 35S-AC2 sustained the GFP fluorescence up to 14 dpi (Fig. 1d). In the second assay, the 35S-AC2 constructs were agro-infiltrated in GFP silenced lines and the reversal of GFP silencing in the infiltrated zones was quantitated in terms of siRNA accumulation and GFP transcript at 3 dpi, 7 dpi and 14 dpi. We observed 6-fold reduction in the level of GFP siRNA in the AC2-infiltrated regions normalized to the vector control from 3 dpi to 14 dpi (Fig. 1e). Conversely, 7 fold increased in the level of GFP transcript from 3 dpi to 14 dpi in the AC2 infiltrated zone was detected (Fig. 1e lower panel). In a separate experiment the 35S-GFP construct was infiltrated in leaves of wild-type and AC2 over-expressing tobacco plants. As expected, we observed greater GFP fluorescence and longer duration of fluorescence in the AC2 expressing line in comparison to the wild-type plants (Fig. 1f). Previously, we have reported the suppression activity of AC2 on virus induced gene silencing using a MYMIV-based viral amplicon vector (Karjee et al., 2008). The expression analysis of small RNAs in this case also showed significant reduction in siRNA levels in the presence of AC2 (Mishra et al., 2014). These results together suggest that AC2 may reduce the accumulation of siRNAs by interfering with a key component of its biogenesis.

MYMIV-AC2 is not an RNA binder

Several RSS exhibit small RNA binding as a common strategy to suppress RNA silencing (Lakatos et al., 2006). To investigate the mechanism of suppression activity by MYMIV-AC2 was whether mediated by small RNA binding, electrophoretic mobility shift assay (EMSA) was performed. In the presence of recombinant MBP tagged MYMIV-AC2 protein, no mobility shift was observed for long ssRNA, long dsRNA, ds 21 nt RNA as well as ss 21 nt RNA (Fig. 2a–c). However, a detectable shift was observed with the positive control B2 protein of Flock house Virus (FHV), another well-known dsRNA binding RSS (Singh et al., 2009). Thus, the suppression activity of MYMIV-AC2 probably does not involve direct binding of small RNA.

MYMIV-AC2 does not interfere with the Dicer activity

Above results clearly indicated that even though AC2 showed no affinity for siRNA binding, it drastically affected siRNA accumulation, suggesting it might interfere with siRNA biogenesis itself. The RNase III enzyme Dicer is one of the prime components in siRNA biogenesis (Tang et al., 2003; Kurihara and Watanabe, 2004; Xie et al., 2004) so the effect of MYMIV-AC2 on Dicer activity was studied *in vitro*. The wheat germ extract based *in vitro* dicing assay was carried out in presence of MYMIV-AC2 at the protein amount of 0–1.32 μg but no visible difference was detected in the generation of ~21 nt small RNA from the radiolabelled dsRNA substrate (Fig. 2d). This indicated that AC2 did not affect the dicing activity. However, the FHV-B2 protein, which was taken as the positive control for assay mentioned above, showed a significant reduction in the small RNA generation that increased proportionally with the amount of the exogenous B2 protein

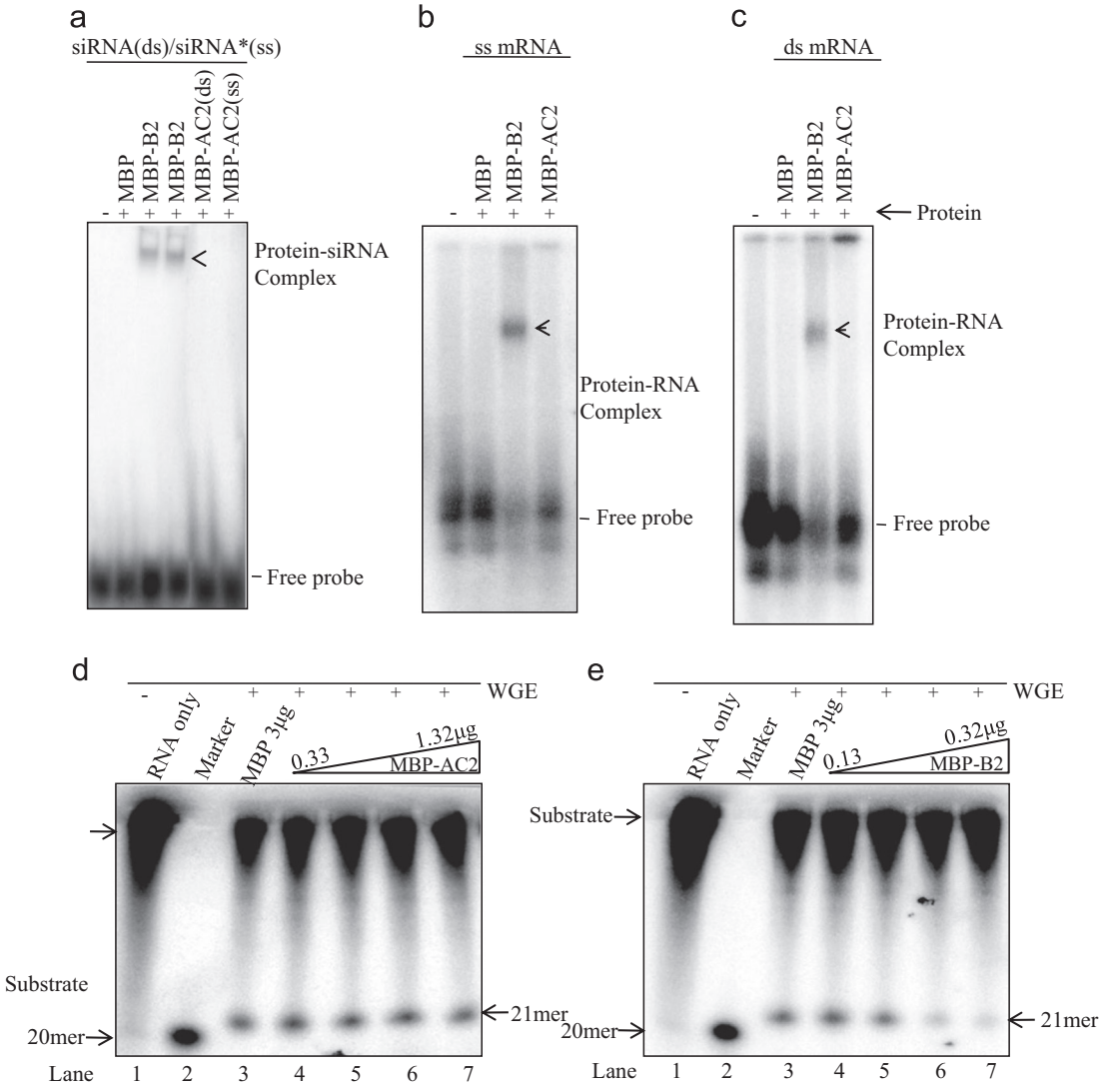

Fig. 2. MYMIV-AC2 does not bind to any of the RNA species and does not inhibit the hpRNA cleavage in wheat germ extract (WGE). Electrophoretic mobility shift assays using purified MBP-AC2 (MYMIV) and MBP-B2 (FHV) fusion proteins and (a) synthetic siRNA (ds)/siRNA* (ss), (b) *In vitro* transcribed radiolabeled ssRNA, (c) dsRNA as indicated at the top of each blot. The Arrows indicate protein-RNA complexes that were analyzed by 6% native PAGE. The last two panels show autoradiograph of 15% denaturing PAGE showing the separation of radiolabeled hpRNA incubated with WGE in presence or absence of (d) MYMIV-AC2 and (e) MBP-FHV-B2. Lane: 1, radiolabeled hpRNA; Lane: 2, DNA Marker (20 mer); Lane: 3, cleavage of hpRNA in WGE; Lane: 4, MBP protein as a negative control; Lanes 5–7, increasing concentration of suppressor.

(Fig. 2e). This showed that the inhibitory effect of AC2 on siRNA biogenesis is not due to interference with the dicing activity.

MYMIV-AC2 interferes with the biogenesis of siRNA by interacting with RDR6

To search for the potential RNA silencing factors that might interact with MYMIV-AC2, phage display assay was carried out. We screened for MBP-AC2-interacting peptides using a randomized phage display peptide (12-mer) library, and the interacting peptides are listed in Table 1. Similarly, the randomized phage display peptide (12-mer) was also assayed using MBP protein alone to normalize the results. The peptide sequences selectively identified from this screen were searched against the *Arabidopsis* database. To qualify as a positive interaction, a minimum stretch of 5 amino acids of interacting peptide must be identical with *Arabidopsis* protein. After eliminating the proteins common in both MBP-AC2 and MBP, we found that AC2 can potentially interact with~ 338 candidate host proteins. These interacting proteins are involved in different biological function such as replication, auxin signaling, disease resistance and RNA silencing. Interestingly, AC2 potentially interacted with key components involved in different steps of RNA silencing pathway (Table 2).

The AGO1-peptide sequence (P13) and RDR6-peptide sequence (P20) were over represented, while other peptides occurred either uniquely or 4 times at most in the screening assay. The P13 peptide matched aa 130–137 (AtAGO1$_{130-137}$) while another peptide, P20, matched aa 970–974 (AtRDR6 $_{970-974}$) in *A. thaliana* AGO1 and RDR6, respectively (Tables 2 and 3).

RDR6 was identified as one of the potential interacting partners of AC2 in the phage display screen. RDR6 is involved in the biogenesis of siRNA from the sense gene or a structured region of viral RNA, by generating dsRNA. To further confirm the interaction of MYMIV-AC2 and AtRDR6, *in vitro* co-immunoprecipitation was performed using recombinant purified proteins. *In vitro* translated radiolabelled RDR6 was mixed with purified MBP-tagged MYMIV-AC2 and immunoprecipitated using beads coated with anti-AC2 antibody. The supernatant as well as bead eluent was run on SDS-PAGE and analyzed/quantitated for the radioactive band present in the blot using phosphorimager. The ~130 kDa band corresponding to the RDR6 was obtained in eluate along with that of MYMIV-AC2 (Fig. 3a lane 8). The shorter version of AC2, *i.e.*, AC2$_{\Delta 91-136,}$ which

lacks the RNA silencing-suppression activity failed to precipitate the radiolabel in the same assay (Fig. 3a, lane 6). Thus, this confirmed the direct interaction between the MYMIV-AC2 and RDR6.

It has previously been shown that *Arabidopsis* RDR6 possess terminal nucleotidyl transferase activity as well as primer-independent RNA polymerase activities on single-stranded RNAs (Curba and Chen, 2008). In our previous experiment we observed reduced accumulation of siRNAs produced by sense transgene and established RNA silencing in the presence of AC2. Moreover, AC2 directly interacts with *At*RDR6. These findings led us to hypothesize that AC2 interacts with RDR6 and in turn, inhibits the RDR6 catalyzed RNA polymerase activity on single-stranded RNA. To test this hypothesis, we investigated the efficacy of RDR6 catalyzed RNA polymerase activity in the absence or presence of AC2 *in vitro*. The RDR6-catalyzed RNA polymerization reactions were performed *in vitro* using 105 nt long ssRNA (RNA without Cap and ploy A tail) as a template, in the presence or absence of AC2 (Fig. 3d, e). It was observed that template directed RNA synthesis, *i.e.*, the copying reaction of RDR6 protein derived from the baculo-expression system (Fig. 3c), was perfectly normal as the copied strand was of desired size (Fig. 3d, lane 3). This band was not detected when CTP was omitted in the copying reaction, implicating that the band was the product of RNA replication and not of nucleotidyl transferase activity. But this copying power was reduced in presence of 25 ng of AC2 (Fig. 3d, lane 5). The inhibitory effect increased with increasing amount of AC2 protein and 150 ng AC2 was sufficient to nearly abolish the RDR6 activity completely (Fig. 3d lane 8). Our result (Fig. 3d, f) suggested that the activity of 100 ng of RDR6 (130 kDa) was inhibited (about 60%) by 100 ng of MBP-AC2 (65 kDa), In other words, 2 molecules of AC2 are perhaps sufficient to annul the activity of 1 molecule of RDR6. In presence of $AC2_{\Delta 91-136}$ (RSS negative), no effect was seen on the RDR6 activity even at a high protein amount of 200 ng (Fig. 3d lane 9 and Fig. 3e, lanes 5–7). Similarly no effect was observed on using the tags alone (Fig. 3d lane 4, Fig. 6e lane 4). This demonstrates that interaction with MYMIV-AC2 inhibits the RDR6 activity.

Based on the results it was hypothesized that RDR6 knockdown should mimic the effect of AC2 suppression activity in reversing the silencing of reporter gene. The *in planta* assay included agro-infiltration of 35S-GFP with 35S-hpRDR6 (RDR6IR) or 35S-AC2. The GFP expression was monitored 6, 10 and 12 dpi by visualizing under UV. GFP co-infiltrated with empty vector ceased to express green fluorescence by 10 dpi, while the GFP co-infiltrated with AC2 or RDR6-IR showed analogous expression with the fluorescence levels increasing up to 12 dpi (Supplement Fig. 1). These results clearly demonstrate phenotypically that MYMIV-AC2 suppression mechanism follows the pathway of inhibition of RDR6 activity which might in turn affect the siRNA biogenesis.

Table 1
List of peptide sequences obtained from phage display library screening against MYMIV AC2 protein. The 12-mer peptide sequences are designated as 'P' followed by numbers. The values within the parentheses represent the frequency of occurrence of the peptides in the screening.

P1 [1]	P16 [1]	P31 [1]
TMASSMWPLNRW	APAARDTGLSPM	GHKMHNVAPSIQ
P2 [1]	P17 [1]	P32 [1]
DHASTWMVKRGV	TTPPPTTMHSAR	NFSQPPSKHTRS
P3 [1]	P18 [1]	P33 [1]
DLNYFTLSSKRE	KAMSPGMALSVS	STFGTSRAPLSN
P4 [1]	P19 [1]	P34 [1]
TPVLETPKLLLW	SNPIILPTPYPN	NWNAGKGTMSPP
P5 [1]	P20 [12]	P35 [1]
NPQYARSQLQPV	SLPNGNKPKLYV	AAPMPLNGVPP
P6 [1]	P21 [1]	P36 [1]
YGTRLNSTHWPY	VLTTTYPRPQLL	SHTGASTSKITL
P7 [1]	P22 [1]	P37 [4]
HVKKQVWAASTR	SYKTGFESRKPL	NSMIAHNKTRMH
P8 [1]	P23 [1]	P38 [1]
DATRHLTELALP	QSFLVLNQLHSH	EHLRMHSGHYFT
P9 [1]	P24 [1]	P39 [1]
QTILQGPQSFSS	YMSSPDRQPTLT	KAMSPGMALSVS
P10 [1]	P25 [1]	P40 [1]
ASTSGAWAAHKI	NTYTPFPGALPM	FEPPSLHPELPG
P11 [1]	P26 [1]	P41 [1]
HPTMDTRQTKLA	TMGFTAPRFPHY	IVTDHARSPKLA
P12 [1]	P27 [1]	P42 [1]
FKYQHAEGLLPT	NWNAGKGTMSPP	TSYPPETLRDSP
P13 [17]	P28 [1]	P43 [1]
SSSEPTLSETPA	LSHSTVKAAPNV	TKPSEEANAFRL
P14 [1]	P29 [1]	P44 [1]
APYNLYSGANQP	QYRDHPSTYAGM	SKPSEEANAIWP
P15 [1]	P30 [2]	P45 [3]
GAASRTYLHELI	SAHHYSTTSRPT	HPSQSPSPSTRDPW

Table 2
The list of putative RNA silencing related host factors interacting with MYMIV-AC2 protein identified by phage display library screening method.

RNA Dependent RNA Polymerase 6 (RDR6)
Dicer-like 1 (DCL1)
Argonaute 1 (AGO1), Argonaute 2 (AGO2) and Argonaute 7 (AGO7)

MYMIV-AC2 abrogates the tasi-RNA formation in-planta in transient assay

As depicted in the Fig. 4, tasiRNAs are generated from non-coding transcripts through Argonaute 1/7 mediated and miRNA guided cleavage, followed by conversion to double stranded RNA by the RNA-dependent RNA polymerase and suppressor of gene silencing 3 (SGS3) (Talmor-Neiman et al., 2006). The resulting dsRNA is further processed by dicer-like enzyme 4 (DCL4) to produce a phased array of 21-nt siRNAs starting at the miRNA cleavage site (Xie and Qi 2008; Allen et al., 2005). RDR6 is a one of the major components in the tasiRNA biogenesis. Thus, we wanted to investigate if the ectopic expression of AC2 would inhibit the tasiRNAs biogenesis (Fig. 4b). To this end, we agro-infiltrated AC2 or the empty vector in the leaves of wild type *N. benthamiana.* We isolated the total RNAs from the agro-infiltrated zone 6 dpi and probed against the native tasiRNAs. Unfortunately, the level of native tasiRNAs was found to be below detection level. This

Table 3
Portions of the *At*AGO1 and *At*RDR6 sequences

AGO1 (*Arabidopsis thaliana*)
MVRKRRTDAPSEGGEGSGSREAGPVSGGGRGSQRGGFQQGGGQHQGGRGYTPQPQQGRGGRGYGQPPQQQQQYGGPQEYQGRGRGGPPHQGGRGGYGGGRGGGPSSGPPQRQSVPELH
QATSPTYQAVSSQPTLSEVSPTQVPEPTVLAQQFEQLSVEQGAPSQAIQPIPSSSKAFKFPMRPGKGQSGKRCIVKANHFFAELPDKDLHHYDVTITPEVTSRGVNRAVMKQLVDNYRDSHL
GSRLPAYDGRKS

RDR6 (*Arabidopsis thaliana*)
YDAAEEKTLGRAVNHQDIIDFFARNMANEHLGTICNAHVVHADRSEYGAMDEECVLLAELAATAVDSPKTGKIVSMPFHLKPKLYPDFMGKEDYQTYKSSKILGRLYRRVKEVYDEDAEASSEE
SSDPSDIPYDIDLEIPGFEDLIPEAWGHKCSYDRQLIGLLGQYKVQKEEEIVTGHIWSMPKYTSKKQCDLKERLKHSYNSLKKEFRKVFEETILDHEELSEEEKNILYEKKA

Interacting peptide regions are underlined.

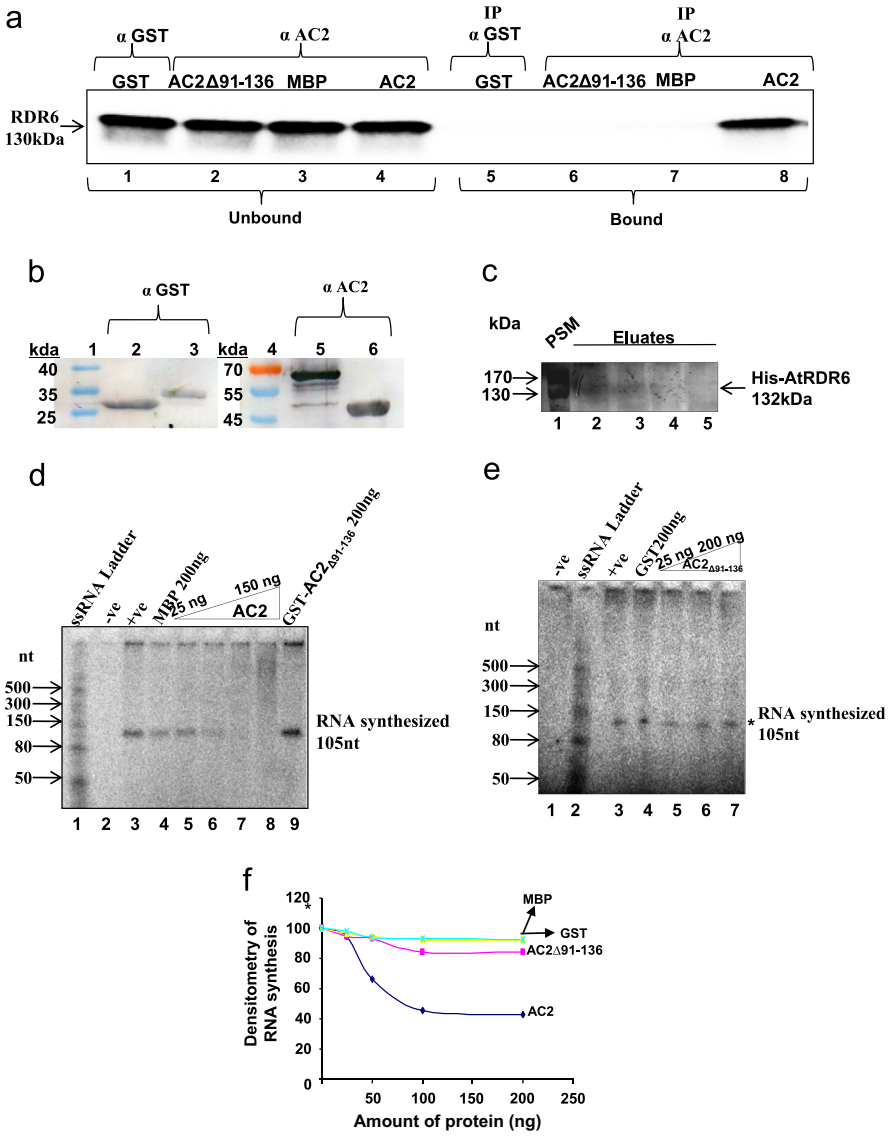

Fig. 3. AC2 interacts with RDR6 and inhibits the RDR6 activity *in vitro*. (a) Coimmunoprecipitation of AC2 and *in vitro* translated radiolabeled *At*RDR6. GST-AC2$_{\Delta 91-136}$ and RDR6 were mixed and immunoprecipitated (IP) with polyclonal antibody GST (lanes 1, 2, 5 and 6). MBP-AC2 and RDR6 were mixed and immunoprecipated (IP) with polyclonal antibody AC2 (Lanes 3, 4, 7 and 8). The coimmunoprecipitate was separated on 10% SDS-PAGE and autoradiographed. RDR6 was coimmunoprecipitated with AC2 (lane 8) but not with GST-AC2$_{\Delta 91-136}$ (lane 6). MBP and GST proteins alone were used as negative controls (lane 7 and lane 5, respectively). A fraction (1/3) of radiolabeled reaction mixtures were loaded on the left panel (unbound lanes 1–4). (b) Western blot of GST (lane 2), GST-AC2$_{\Delta 91-136}$ (lane 3) and MBP (lane 6), MBP-AC2 (lane 5) with polyclonal antibody GST and AC2 respectively. Lane 1 and 4 show the prestained protein marker. (c) Western blot of His-RDR6 protein purified from insect cells using anti-His antibody. Lane 1 is prestained marker and the respective sizes are indicated by arrow on the left. Lanes 2–5 are the eluates of His-RDR6 and its molecular weight is shown by arrow in right. (d) Complementary RNA strand synthesized by His-RDR6 from ssRNA template was resolved by denaturing polyacrylamide gel electrophoresis. The size of the synthesized RNA is 105 nt indicated by asterisk. Lane 1 is the radiolabelled ssRNA ladder and different size is indicated by arrows. Lane 2 is negative control where His-RDR6 was not added in reaction. Lane 3 represents the cRNA strand synthesis in the presence of His-RDR6. Lane 4 is the RDR6 activity in the presence of highest concentration of MBP (Fusion tag of AC2 protein). Lanes 5–8 are the RDR6 activity in the presence of different concentration of AC2. Lane 9 showing the RDR6 activity in the presence of highest concentration of AC2$_{\Delta 91-136}$. (e) Lane 1 showing no RDR6 activity when His-RDR6 was not added in reaction. Lane 2 is ssRNA ladder. Lane 3 showing RDR6 activity. Lane 4 is RDR6 activity in the presence of highest amount of GST (Fusion tag of AC2$_{\Delta 91-136}$). Lanes 4–7 showing the RDR6 activity in the presence of different concentration of AC2$_{\Delta 91-136}$. (f) Plot showing the band intensity of RNA synthesis in presence of various protein concentrations.

motivated us to construct a pCAMBIA-2300 based vector where a Multiple Cloning Sites (MCS) was inserted downstream of 35S and the MCS was immediately flanked by two binding sites (5′ BS & 3′ BS) of miR-390, a conserved miR within the plant kingdom (TAS vector, Fig. 4a). When such a vector is introduced in plants, the tasiRNAs are expected to be generated in plants from any transcribing DNA sequence cloned within the MCS (Wang et al., 2005). Indeed we observed the generation of AC4 specific siRNAs when the AC4 DNA sequence of MYMIV was cloned at the MCS (TAS-AC4) in transient assays performed in wild type *N. benthamiana.* The siRNA formation was completely abolished following mutation at the 9–12th position starting from 5′ to 3′ miR-390 binding site (5′ BS) in the flanking regions (data not shown, separate communication). Taken together, this result clearly suggested that TAS-AC4 vector is perfectly capable of synthesizing AC4 specific tasiRNAs in wild type *N. benthamiana*.

As the biogenesis of tasiRNAs requires functional RDR6 activity, we wanted to study the effect of ectopically expressed AC2 on the generation of tasiRNAs in transient assay. TAS-AC4 vector was agro-infiltrated in the presence of pBI121-AC2, or the empty vector pBI121, or pART-hpRDR6. The total RNAs were isolated from the infiltrated zones at 6 dpi followed by visualization of 22 mer AC4 specific tasiRNAs by autoradiography in northern blot (Fig. 4c). The quantities of the small RNAs were measured by phosphorImager

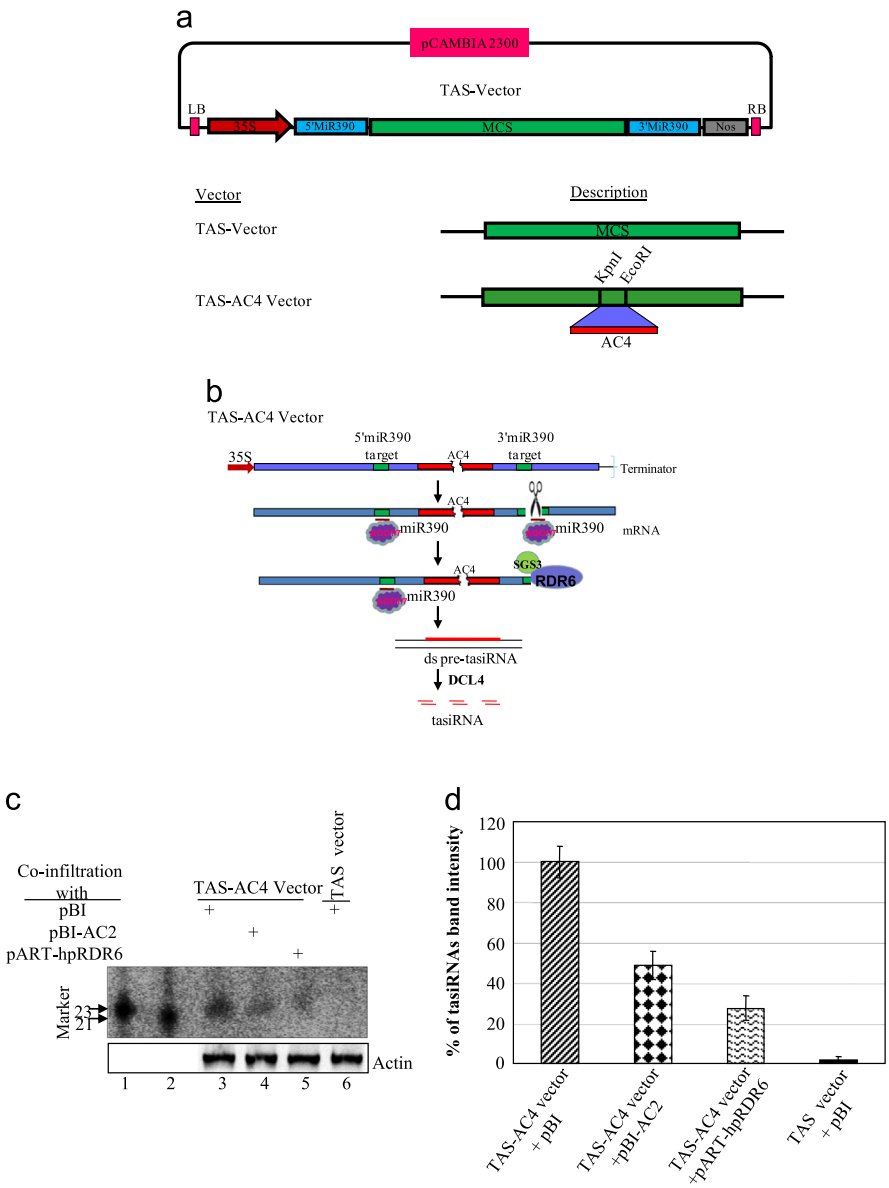

Fig. 4. AC2 blocks the biogenesis of tasiRNA *in planta*. (a) Showing schematic diagram of construction of TAS vector and TAS-AC4 vector respectively. (b) Schematic representation of biogenesis of tasiRNA. (c) Small RNA blot analysis of 20 μg leaves RNA from agroinfiltrated area with different combinations mentioned on the top of gel. The blot was hybridized with radio-labeled MYMIV-AC4 DNA probe (complementary to tasiRNA) and actin served as an internal control. (d) Graph was plotted with % of biogenesis of tasiRNA normalized with actin control and different combination of constructs used during agro-infiltration.

following normalization by actin control. The band intensity of tasiRNAs is plotted in Fig. 4d. The biogenesis of tasiRNAs was greatly reduced by expression of either by AC2 or hpRDR6 (RDR6-IR). Such down regulation of the generation of tasiRNAs by AC2 also points towards an *in vivo* interaction between RDR6 and AC2.

MYMIV-AC2 interacts with AGO1 and suppresses RNA silencing by direct blocking of RISC activity in vitro

RDR6 has specific role in sense gene mediated silencing but not in dsRNA triggered silencing. Thus, if RDR6 inhibition is the sole mechanism for the suppression activity of MYMIV-AC2, it should be ineffective against the dsRNA triggered silencing. Wang et al. (2005) found that AL2 and L2 proteins can suppress GFP-directed silencing in the transient system. To this end, *N. benthemiana* leaf tissues were co-infilterated with agrobacterium cultures delivering Ti plasmids expressing GFP, dsGFP and AL2/L2. Interestingly, we also observed that AC2 can suppress GFP-directed silencing in the transient system (data not shown). This suggested that AC2 might suppress another additional pathway that does not involve the RDR6-dependent activity.

In the phage display assay with MYMIV-AC2 bait (Tables 2 and 3), *At*AGO1 was also present as one of the interacting partners. Hence, we examined if AC2 could exert its influence by inhibiting the siRNA function at the RISC step. First, to validate this interaction *in vitro* and *ex vivo*, co-immunoprecipitation and yeast two-hybrid analysis were performed. For the *in vitro* co-immunoprecipitation assay, the wheat germ extract was enriched with the *in-vitro* produced, radiolabelled AGO1 and subsequently incubated with recombinant MBP-AC2. The immunoprecipitation (IP) was done with polyclonal antibody raised against MBP-AC2. This pool of antibodies was eventually made free of MBP-antibody by adsorption against the MBP protein. The immunoprecipitate was run on SDS-PAGE, blotted and autoradiographed. The autoradiogram showed the presence of AGO1 (Fig. 5a, lane 5) while no detectable band was observed with the tag alone (MBP) as negative control (Fig. 5a, lane 6). This result shows the physical

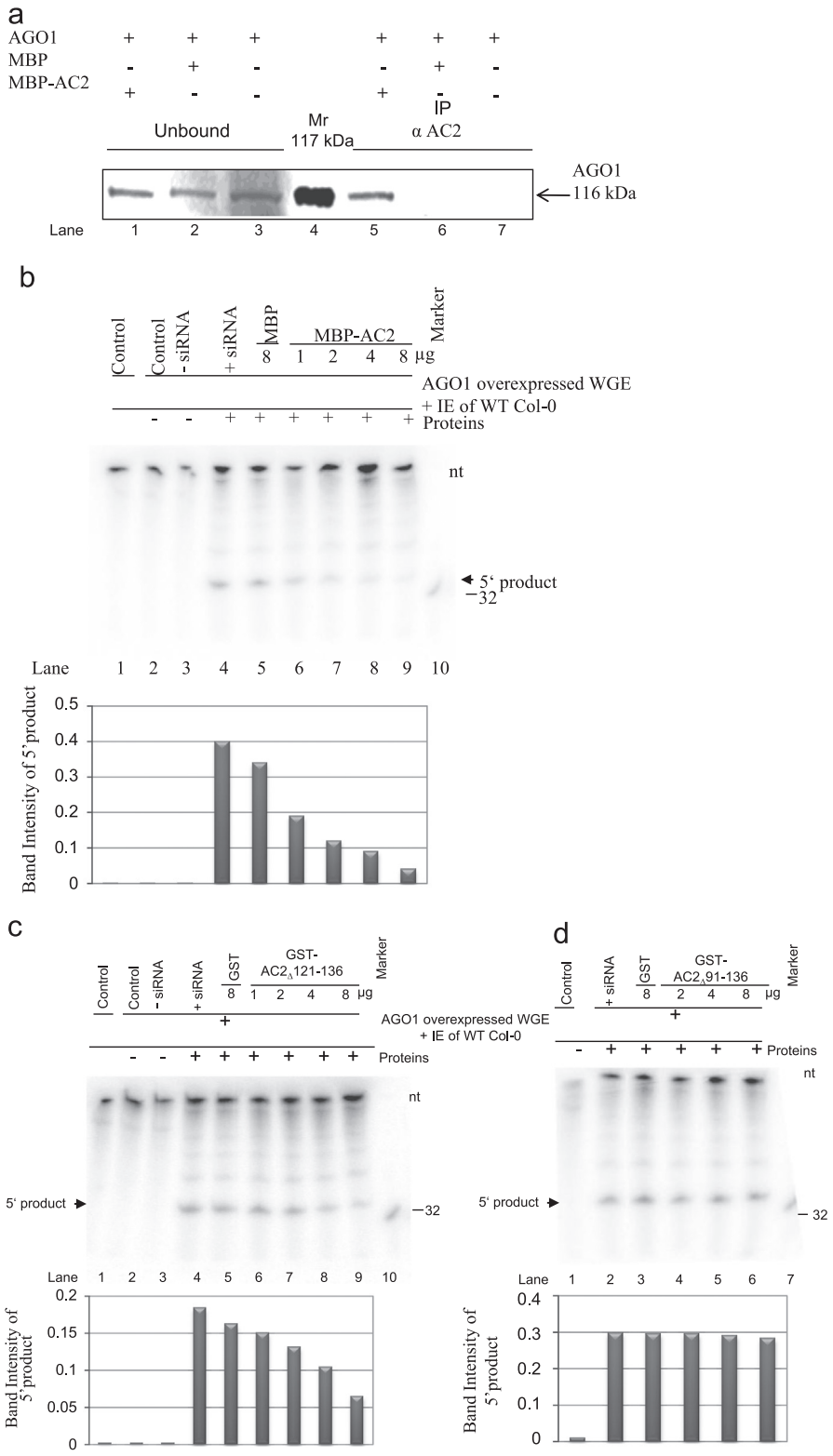

Fig. 5. AC2 interacts with AGO1 *in vitro* and blocks the activity of RISC. (a) Co-immunoprecipitation of MBP-AC2 and *in vitro* translated labeled *At*AGO1. AC2 and AGO1 were mixed and immunoprecipitated (IP) with polyclonal antibody AC2 (it shows cross reaction with MBP as antibody raised against MBP-AC2). The co-immunoprecipitate was separated on 10% SDS-PAGE and autoradiographed. AGO1 co-immunoprecipitates with AC2 (lane 5), MBP protein was used as a negative control (lane 6). A fraction (1/3) of radiolabeled AGO1protein was loaded on the left panel (input lanes 1–3). Lane 7 shows that AGO1 does not bind to protein A sepharose. Mr. denotes marker (lane 4). (b–d) *In vitro* slicing assay in presence of full length or deletion mutants of AC2.Wheat germ extract containing overexpressed AGO1 mixed with 1 µg/µl of inflorescence extract (IE) of wild type *Arabidopsis* Col-0 in absence and presence of siRNA respectively (lane 3 and 4). The mixture was incubated with the indicated suppressor protein (lanes 6–9) or control protein (lane 5) before mixing with siRNA complementary to the target GFP mRNA. Reconstituted RISC was tested for cleavage activity by incubation with a 32p internally labeled GFP mRNA. RNAs recovered from the reactions were fractionated on 12% denaturing gels. The position of intact substrate, 5′ cleavage product, and markers are shown. In each experiment, the cleavage efficiency was normalized to that obtained in the presence of siRNA.

Table 4
AC2 protein interacts with AGO1 in yeast two-hybrid system[a].

Bait	Prey	Interaction[b]
AGO1	AC2	+++
AGO1	AC2$_{\Delta}$121–136	+
AGO1	AC2$_{\Delta}$91–136	–

[a] The indicated bait protein was expressed as GAL4 DNA-binding domain fusion, and prey proteins were expressed as GAL4 activation domain fusions in yeast AH109 cells.

[b] Interaction was indicated by the ability of cells to grow on medium lacking His and containing 5 mM 3-aminotriazole. As an additional indicator of interaction, colonies were monitored for LacZ activity (blue color) using a filter-lift assay. Interaction symbols are as follows: – , no interaction, no evidence of blue color after overnight incubation; +, interaction, blue color developed within 2 to 6 h.

interaction of AGO1 and AC2 *in vitro*. Similarly, the yeast two-hybrid analysis further confirmed the interaction of AGO1 with AC2 *ex vivo*. It was observed that the RNA silencing suppression proficient mutant AC2$_{\Delta 121-136}$ interacted well with AGO1, while the silencing suppression negative mutant AC2$_{\Delta 91-136}$ failed to do so (Table 4). These experiments thus confirmed the interaction between the MYMIV-AC2 and *At*AGO1.

To determine the significance of this specific interaction, *in vitro* slicing assays were performed with AC2, AC2$_{\Delta 121-136}$ and AC2$_{\Delta 91-136}$. RISC was reconstituted by mixing *Arabidopsis* AGO1 with the WT Col-0 inflorescence extract. To visualize the cleavage activity of the reconstituted RISC, the mentioned mix was incubated with ds siRNA^{GFP} and radiolabelled GFP mRNA. When incubation mixture was resolved on 12% Urea-PAGE gel, an RNA-band of 40 nt, corresponding to the expected size of 5′ cleaved product, was visible in the autoradiogram (Fig. 5b, lane4).

Next, we determined the cleavage activity of the RISC in presence of different amounts of recombinant AC2, AC2$_{\Delta 121-136}$ and AC2$_{\Delta 91-136}$ proteins (Fig. 5, b–d). Since, the investigation is directed to understand the interference of the AC2 with the AGO activity, all the cleavage activity was performed with ds siRNA^{GFP} pre-loaded RISC. This was incubated with the test proteins and radiolabelled GFP mRNA and then followed up for the analysis of the cleaved product. The MYMIV-AC2 and MYMIV-AC2$_{\Delta 121-136}$ showed significant reduction in the cleavage activity in comparison to the MYMIV-AC2$_{\Delta 91-136}$ and tag alone (MBP and GST) (Fig. 5b–d, lanes 5–9). However, the inhibition of the cleavage activity was more potent in MYMIV-AC2 than MYMIV-AC2$_{\Delta 121-136}$. The inhibition activity also showed dose dependent increase with the increasing amounts of the RNA silencing suppressor proteins MYMIV-AC2 and MYMIV-AC2$_{\Delta 121-136}$ (2–8 μg). The *in vitro* slicing assay along with the protein-protein interaction study strongly indicates that MYMIV-AC2 inhibits the RISC activity by interacting with AGO.

Thus, the MYMIV-AC2 makes a binary attack on the RNA silencing pathways involving two steps, one at the upstream RDR6 level with consequent reduction in siRNA biogenesis and second at the downstream AGO1-mediated RISC activity by reducing the function of siRNA.

Discussion

We have previously identified MYMIV-AC2 is a suppressor of RNA silencing. Though suppression of TGS by AC2 proteins has been well studied, the true mechanism of AC2-mediated suppression of PTGS is relatively unknown. The goal of the present study was to investigate another mechanism of AC2-mediated suppression activity.

MYMIV-AC2 interferes with the biogenesis of siRNA

RNA binding has been reported as one of the common suppression strategies of RNA silencing by most of the virus encoded RSS (Lakatos et al., 2006). In order to understand the mechanism of suppression by MYMIV-AC2 we investigated its binding affinity for RNA species. However, the gel shift assay has shown that MYMIV-AC2 did not interact with ss siRNAs and ds RNAs. This observation is in well agreement with the previous study on geminiviruses. There are plant RNA viruses which bind to ssRNA and ds RNA to inhibit RNA silencing. Additionally, we also observed that it does not bind to ss RNA or ds RNA pointing towards the alternate RNA silencing suppression mechanism. Intriguingly, even though the MYMIV-AC2 did not interact with siRNA it was capable of altering the level of siRNA accumulation (Fig. 1e). There is a notion that the class of RSS that fails to bind with siRNAs generally interacts with the host RNAi factors to incapacitate the biochemical functions of the factors. Unlike many other plant viral suppressors, the AC2 protein does not harbor the GW-motif to act as an RNAi suppressor (Giner et al., 2010). Hence we examined if MYMIV-AC2 would interact with any of the host RNAi factors. The phage display analysis identified several proteins including AGO1, DCL1 and RDR6 as the AC2 interacting proteins (Table 3). However, *in vitro* dicing assays did not reveal any inhibitory effect on the dicing activity (Fig. 2). Geminiviruses lack a dsRNA in their life cycle, however secondary structure and convergent of transcript provide dsRNA substrate for DCL activity (Moissiard et al., 2007; Chellappan et al., 2004; Akbergenov et al., 2006). Besides this geminiviruses produce abundant transcripts which could be perceived as aberrant RNAs and served as a template for the host RDRs to produce dsRNAs (Kim et al., 2009). RDR6 is required in siRNA biogenesis during sense gene-mediated silencing and virus induced gene silencing (Qu, 2010; Di Serio et al., 2010; Qu et al., 2005; Schwach et al., 2005; Vaistij and Jones 2009). In addition to this, Suppressor of Gene Silencing 3 (SGS3), a dsRNA-binding partner of RDR6, is required to amplify viral siRNAs that allow plants to combat against virus infection (Chellappan et al., 2004; Garcia-Ruiz et al., 2010; Moissiard et al., 2007; Wang et al., 2011). Previously, it has been reported that Tomato yellow leaf curl virus encoded V2 protein suppresses S-PTGS by direct interaction with SGS3 and competing for binding to dsRNA substrate (Fukunaga and Doudna, 2009; Glick et al., 2008). Recently, Li et al. (2014) reported that TYLCCNV βC1 induced level of Nbrgs-CaM and suppresses the S-PTGS by inhibiting the production of secondary siRNAs, likely through repressing RDR6 expression. Consistent with these studies, it appears that interference with SGS3/RDR6-mediated dsRNA formation is a common mechanism for geminiviral encoded suppressor proteins. However, it is unknown that whether direct interaction of geminiviruses-encoded suppressor proteins and RDR6 is required to suppress RNA silencing. Here we report that a DNA geminivirus-encoded AC2 physically interacts and inhibits the RDR6 activity (Fig. 3). This observation was partly supported by the *in planta* reversal of reporter gene silencing assays, in which RDR6 knockdown mimicked the effect of AC2 suppression activity (Supplement Fig. 1). RDR6 is a conserved protein in the plant kingdom and therefore, we can conclude that the MYMIV-AC2 interfered with the host RDR6 for the suppression activity. As RDR6 is inhibited, the intracellular dsRNA formation and the subsequent siRNA generation would be hampered. This explains the lessening of siRNA accumulation in presence of AC2 (Fig. 1e). This finding has major significance to geminivirus biology, as RdRp generated dsRNA from Rep/AC1template (Chellappan et al., 2004) is one of the possible mechanisms for inducing RNA silencing against the virus.

tasiRNAs are generated from non-coding transcripts through Argonaute 1/7 mediated and miRNA guided cleavage, followed by

conversion to double stranded RNA by the RNA-dependent RNA polymerase and suppressor of gene silencing 3 (SGS3) (Talmor-Neiman et al., 2006). The resulting dsRNA is further processed by dicer-like enzyme 4 (DCL4) to produce a phased array of 21-nt siRNAs starting at the miRNA cleavage site (Xie and Qi, 2008; Allen et al., 2005). RDR6 is a one of the major components in the tasiRNA biogenesis. Therefore it was logical to understand the significance of AC2 and RDR6 interaction *in planta* by investigating the tasiRNA biogenesis. We constructed the pCAMBIA-2300 based TAS-vector that generated atasiRNA like small RNAs using the two-hit models of miR390 in tobacco (Wang et al., 2005). By using this method, we have successfully made tobacco transgenic generating *Tomato leaf curl New Delhi* encoded AC2 and AC4 specific tasiRNA. These transgenic plants were challenged separately against ToLCNDV and Tomato leaf curl Gujarat virus and showed absence of symptom and low accumulation of the corresponding viruses (Singh et al., 2015). The co-infiltration of this vector and the plasmid expressing AC2 protein in tobacco using the agro-infiltration technique reduced the formation of siRNAs (Fig. 4c, d). The siRNAs are generated because of the activity of tobacco RDR6 which is more than 90% identical with *At*RDR6.The ectopic expression of AC2 interfered with the tobacco RDR6 activity, reflecting protein-protein interaction between the concerned proteins and subsequent loss of RDR6 activity. Hence the findings of Fig. 4 are quite in agreement with the proposed *in vivo* interaction between RDR6 and AC2.

MYMIV-AC2 also interferes with the siRNA function by blocking the AGO1-mediated slicing activity

Cucumber mosaic virus is a plant RNA virus which encodes 2b suppressor which interferes with miRNA pathways and abrogates RNA silencing including VIGS by direct interaction with AGO1 and inhibition of its slicer activity (Zhang et al., 2006). Similarly, the Polerovirus silencing suppressor P0 interacts and degrades AGO1 protein to overcome RNA silencing in plant (Baumberger et al., 2007; Bortolamiol et al., 2008). Wang et al. (2005) found that geminiviral encoded AL2 and L2 proteins can suppress dsRNA triggered silencing in the transient system. We also found similar observation in the same set of experiment in the presence of MYMIV-AC2 (not shown). These data reinforced that AC2 might suppress another additional pathway that does not involve the RDR6-dependent activity. Earlier, we found in the phage display assay that AC2 might also interact with *At*AGO1 protein. As AGO1 is primarily involved in slicing of the transcripts, we proceeded to check the influence of AC2 on AGO1. First we confirmed the interaction by two different techniques, namely, yeast two-hybrid approach and co-immunoprecipitation. The two-hybrid

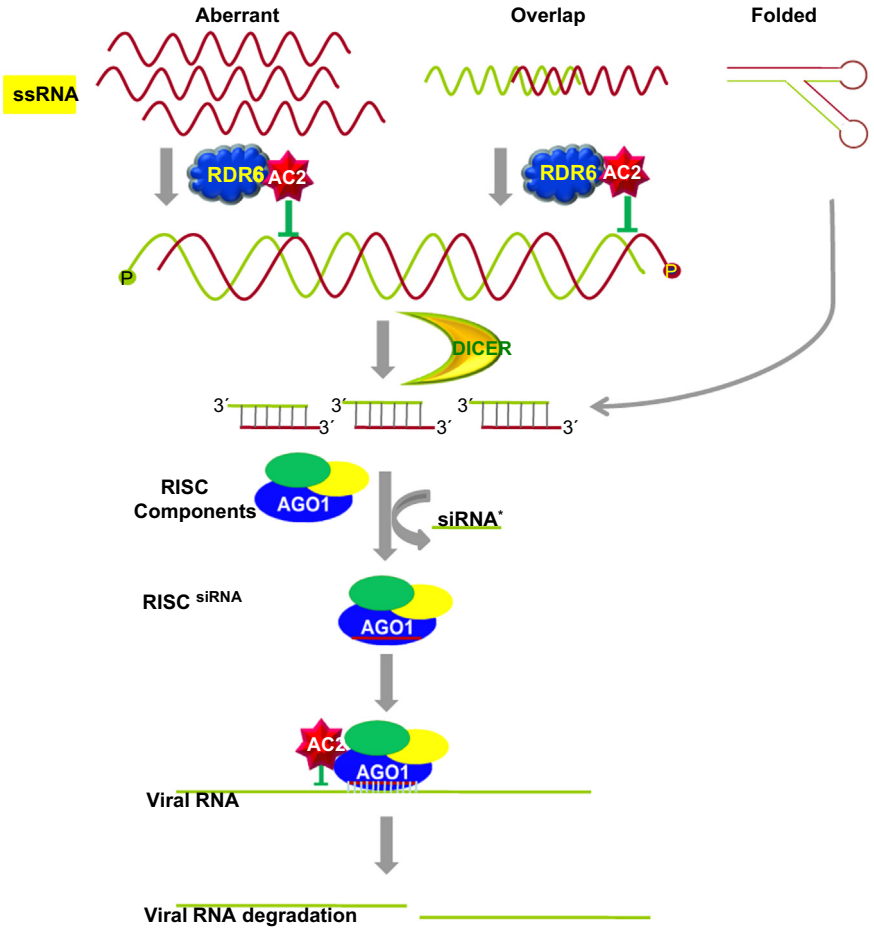

Fig. 6. A model depicting suppression mechanism of AC2 in RNA silencing pathway. RNA silencing pathway is triggered by dsRNAs generated from overlapping, abundant and folded forms of mRNAs. RDR6 converts aberrant ssRNA and overlap RNA in to double strand RNA. An enzyme called DICER cleaves long dsRNA/folded structured RNA into siRNAs. An RNA-induced silencing complex (RISC) then distinguishes between the different strands of the siRNA. The sense-strand (depicted in light green) is degraded. The anti-sense strand (depicted in brown) is used to target genes for silencing. AC2 physically interacts with RDR6 and inhibits its RNA dependent RNA polymerase activity, thus, RDR6 will not able to convert ssRNA to dsRNA leading to inhibition of siRNA biogenesis. Furthermore, AC2 interacts AGO1 protein thus inhibiting the slicing activity of AGO1. AC2 makes two-prong attack by affecting RNA silencing pathway in two steps: one, upstream of the pathway at RDR6 level and second, downstream on the RISC activity by blocking AGO1 activity.

analysis showed that MYMIV-AC2 interacts directly with AGO1. Interaction with AGO1 was observed with the RSS mutant, MYMIV-AC2$_{\Delta 121-136}$, and not with, the suppression negative mutant MYMIV-AC2$_{\Delta 91-136}$ (Table 3). Co-immunoprecipitation data also supported the interaction (Fig. 5a). This observation is in well agreement with study on the interaction of AGO1 with 2b of cucumber mosaic virus (Zhang et al., 2006) and P0 of polerovirus (Baumberger et al., 2007; Bortolamiol et al., 2008). Like CMV 2b, MYMIV-AC2 blocked the slicer activity in RISC reconstitution assays (Fig. 5b, c). Surprisingly, in this experiment, we observed only 5′ cleaved products even though the RNA substrates were body labeled. Here, we speculate that 3′ cleaved product might had been the substrate of exonucleases present in the arabidopsis inflorescence extract.

MYMIV-AC2 transgenic lines show hypermorphic and showed stunting, leaf curling, leaf yellowing, deformed flowering, and sterility phenotypes (Rahman et al., 2012). It is well established that the miRNAs play the key role in tuning the growth and development of plants (Voinnet, 2009), and the viral suppressors interfere with miRNA biosynthesis and function, leading to developmental anomalies (Chapman et al., 2004; Chellappan et al., 2005; Dunoyer et al., 2004; Kasschau et al., 2003; Mallory et al., 2004; Park et al., 2002; Siddiqui et al., 2008). The likely explanation of abnormalities associated with AC2 transgenic could be directly interacting with AGO1 and interfering with miRNA mediated silencing. Moreover, plethora of miRNAs is reported that involved in host defense (Lecellier et al., 2005; Navarro et al., 2006). Inhibition of miRNA pathways might be a common theme for viruses to reprogramme host gene expression to create a favorable environment for their multiplication.

Thus we conclude that the N-terminal domain of MYMIV-AC2 is responsible for its RSS activity. The suppression activity is achieved by inhibiting the RNAi pathway at multiple steps including the blocking the siRNA biogenesis by inhibiting the RDR6 activity and by impairing the AGO1 slicing activity of the RISC (Fig. 6). The possibility of other modes of activity by the suppressor cannot be ruled out at present. The interaction with AGO1 and RDR6 may also influence the biogenesis and/or function of the other small RNA species like miRNA or tasiRNA and this aspect is currently under investigation.

Material and methods

Cloning of AC2 and deletion mutants, plasmid constructs and agroinfiltration

Plant transformation/agroinfiltration constructs were made for the MYMIV-AC2 and deletion mutants. AC2 and deletion mutants were amplified from MYMIV DNA-A (GenBank accession number AF126406) using combinations of primers listed below. PCR amplified product size of AC2, AC2$_{\Delta 121-136}$, AC2$_{\Delta 111-136}$, AC2$_{\Delta 91-136}$, and AC2$_{\Delta 1-120}$ was obtained as 411 bp, 360 bp, 330 bp, 270 bp, and 51 bp, respectively.

AC2 Fwd 5′-AATTGGCATGCGGAATTCTACACCCTC-3′, AC2 Rev 5′-TTAAGAGCTCTT ACGGAAGATCGATAAGAT C-3′, AC2$_{\Delta 121-136}$ Rev 5′AAgTCgACTTACCAgTgCTTTCTT CAAC-3′, AC2$_{\Delta 111-136}$ Rev 5′AAgTCgACTTACCAgTgCTTTCTTCAAC-3′, AC2$_{\Delta 91-136}$ Rev 5′AAgTCgACTTAgACTCTgCTAgAATTgg-3′, AC2$_{\Delta 1-120}$ Fwd 5′GTCGTCGACAGCTTCAAGTCCAGGAAG-3′.

The cloning was done using *Xba*I or *Bam*HI in the forward primer and *Sac*I in the reverse. The vector pBI121 (Clontech, Palo Alto) was digested with the same pair of restriction enzymes resulting in a fall-out of 1.8 kb GUS gene. *Agrobacterium tumefaciens* (strain LBA4404) constructs were grown in YEM broth under kanamycin antibiotic selection (50 mg/ml) at 30 °C, 250 rpm till the OD reaches 0.8–1.0 at λ_{max}=600. Cultures were harvested at 3000 rpm for 5 min and re-suspended in fresh YEM broth without antibiotic. The homogenous culture was taken in 5 ml needleless syringe and infiltrated the selected young leaf by generating a vacuum with the help of a finger on the dorsal side of leaf and mouth of the syringe on the ventral side. Each agro-infiltrated leaf was labeled for the construct used for this assay.

RNA isolation and northern blot analysis

Total RNA from young leaves was extracted using TRIzol reagent (Invitrogen, Carlsbad, CA, USA) following the manufacturer's instructions. For northern blot analyses, 20 μg of total RNA was separated by electrophoresis on a 1% formaldehyde agarose gel and blotted to a Hybond-N nylon membrane (Amersham Biosciences, Amersham, UK). Blots were hybridized with [α^{32}P] dCTP-labeled mGFP or MYMIV-AC2 probe. For GFP-siRNAs northern blot analysis, enrichment of low molecular weight RNAs was achieved by adding polyethylene glycol (PEG, MW=8000) and NaCl to a final concentration of 5% and 0.5 M, respectively. They were separated on a 15% polyacrylamide 7 M urea gel, transferred to Hybond-N nylon membranes and probed with mGFP RNA.

Cloning, expression and purification of recombinant MBP and GST fusion proteins

AC2 and deletion mutants were purified as described previously (Malik et al., 2005). Briefly, AC2 and deletion mutants amplified (described above) and cloned into *Bam*HI and *Sal*I digested pMal-c2x (New England Biolabs, Ipswich, MA) and pGEX-4T-1 (GE Healthcare, Little Chalfont, UK). Following the manufacture's protocol, MBP fusion protein and GST fusion proteins were purified by affinity chromatography with amylose resin (New England Biolabs (NEB), Ipswich, MA) and glutathione sepharose (GE Healthcare, Little Chalfont, UK), respectively.

In vitro transcription

In order to perform electrophoretic mobility shift assay (EMSA), *in vitro* RISC reconstitution and RDR6 catalyzed RNA polymerization assay, *in vitro* RNA was synthesized according to Promega's manual instructions (Promega, Fitchberg, USA). The 50 μl reaction mixture consists of 5 μl of template DNA (1 mg/ml in water or TE buffer), 10 μl transcription optimized 5X buffer, 5 μl Dithiothreitol [(DTT) 100 mM], 50 U Recombinant RNasin Ribonuclease inhibitor, 10 μl nucleotides (2.5 μl each of 10 mM rATP, rCTP, rUPP plus 2.5 μl 1 mM rGTP), 5 μl Ribo m^7 G cap analog (5 mM), 40 U T7 or SP6, volume was made up by adding nuclease free water. Reaction was incubated at 37 °C for 1 h followed by DNase I treatment for 15 min at 37 °C. Here, 1 μl of DNase I was taken for every 1 μg of template DNA. RNA was isolated by adding 250 μl of TRIzol (Invitrogen, Carlsbad, CA, USA) and 50 μl of chloroform. Free nucleotides were removed by passing the sample through a G-25 microspin column (GE Healthcare, Little Chalfont, UK). Radiolabeled RNA counts were measured by scintillation counter.

Radiolabeled siRNAs and dsRNAs preparation and electrophoretic mobility shift assays (EMSAs)

siRNA^{GFP}(Dharmacon, Lafayette, CO, USA) were phosphorylated using T4 polynucleotide kinase [(PNK), NEB, Ipswich, MA]. siRNAs were 5′ end-labeled with [γ-^{32}P] ATP. Briefly, 15 μM siRNA was incubated in a 30 μl of reaction volume containing 1 × PNK buffer and 10 U of PNK (10U/μl) containing 5 μl (50 μCi) of [γ-^{32}P] ATP (6000 Ci/mmol, Perkin-Elmer Life Sciences, USA). The phosphorylation reactions were incubated at 37 °C for 1 h followed by

purification using G-25 microspin column. Radiolabeled single strand (ss) mRNA of GFP was synthesized using an *in vitro* transcription kit from GFP cloned in pGEMT-Easy vector (Promega, Fitchberg, USA). The reaction was performed in 50 μl of volume using 5 μg DNA with T7 and SP6 RNA polymerase to obtain sense as well as antisense RNA. Double strand (ds) RNA was obtained by incubating sense and antisense mRNA at 90 °C and allowing the temperature to reach at room temperature. EMSAs were done as follows: 2–10 μg suppressors or control proteins and 50,000 counts per minute (cpm) either siRNA or ss mRNA or dsRNA were incubated in 15 μl of binding buffer (0.1 M KCl, 25 mM HEPES, 10 mM DTT at pH 7.5) for 15 min at room temperature. The mixture was then separated on a 15% or 6% native gel.

In vitro dicing assay

To obtain the hair pin RNA (hpRNA), N-terminal 400 bp of GFP was first cloned in pHANNIBAL RNAi vector (CSIRO, Australia) in sense and antisense orientation (detail cloning strategy discussed in other section of materials and methods). Then, for *in vitro* transcription the full cassette was digested with *Xho*I site and cloned in the same site present in the multiple cloning sites (MCS) of pSGI mammalian vector. It has T7 promoter site at the N terminal. Radiolabeled hpRNA of GFP was synthesized using an *in vitro* transcription kit. The reaction was performed in 50 μl of volume using 5 μg DNA with a T7 RNA polymerase. 50,000 cpm internally [α-^{32}P] UTP-labeled hpRNA was incubated in a 10 μl reaction containing 5 μl wheat germ extract (Promega, Fitchberg, USA), 100 μM GTP, 500 μM ATP, 10 mM creatine phosphate, 10 μg/ml creatine phosphokinase, 5 mM DTT, and 0.1 U/μl RNasin (Promega, Fitchberg, USA) at 25 °C for 3 h. Cleaved products were isolated by TRIzol and products were precipitated with 3 volumes cold ethanol in the presence of 20 μg/μl glycogen. The products were further analyzed by electrophoresis in a 15% urea polyacrylamide gel.

Phage display assay

Ph.D.-12 phage display library kit (NEB, Ipswich, MA) was used to analyze the various peptides that interact with AC2 protein. The protocol was followed as per the company instructions. In brief, panning was carried out by incubating a library of phage-displayed peptides with a plate coated with the MBP-MYMIV-AC2 or MBP, washing away the unbound phage, and eluting the specifically bound phage. The eluted phage is then amplified and taken through additional binding/amplification cycles to enrich the pool in favor of binding sequences. After three rounds, individual clones are characterized by DNA sequencing. The sequences of peptides were analyzed by 'BioEdit' software and peptides common in MBP-AC2 and MBP interacting peptides were removed. Each peptide sequence thus obtained was then searched for homologous regions against the non-redundant protein database at NCBI through 'blastp' program adjusted for small sequence analysis. Proteins showing a minimum of five continuous amino-acid matches were short listed as potential candidates for further analyses.

In vitro translation of RDR6 and AGO1

The full length *At*RDR6 and *At*AGO1 genes were amplified by PCR with Platinum Taq Polymerase (Invitrogen, Carlsbad, CA, USA) from cDNA of *Arabidopsis* using gene specific primers. The PCR amplified products were first cloned into TOPO-TA cloning vector (Invitrogen, Carlsbad, CA, USA). The full length *At*RDR6 was taken out from TOPO-*At*RDR6 clone digested with *Eco*RI and *Sal*I enzymes and then cloned into pSGI vector linearized by *Eco*RI and *Xho*I enzymes (as enzymes *Sal*I and *Xho*I are compatible with each other). Similarly, *At*AGO1 was cloned in the pSGI vector linearized by HindIII and SalI enzymes. Each construct was *in vitro* translated using the TnT T7/SP6 Coupled Wheat Germ Extract System (Promega, Fitchberg, USA). The reaction was performed according to product instructions. [^{35}S] methionine radiolabelled proteins were electrophoresed on 10% SDS-PAGE followed by drying the gels in a gel drier and visualized using the phosphorImager (Amersham Biosciences, Amersham, UK).

Immunoprecipitation of MYMIV-AC2 with AGO1 and RDR6 complex

In vitro translated *At*RDR6/AGO1 proteins were incubated with purified MYMIV-AC2 recombinant protein or with other control proteins in a binding buffer (10 mM Tris–Cl pH 7.5, 100–200 mM NaCl, 5 mM $MgCl_2$ and 0.2% BSA) for 30 min at room temperature. After incubation, anti MYMIV-AC2 or control antibody was added and the reaction was kept for 30 min at room temperature on a rocker. The reaction mixture was incubated with protein A-Sepharose 4B (GE Healthcare, Little Chalfont, UK) at room temperature for 30 min on a rocker. Following incubation, the protein A-Sepharose beads were washed thrice with wash buffer (10 mM Tris–Cl, pH 7.5 and 2 mM EDTA). The beads were resuspended in SDS sample buffer containing β-ME and incubated at 95 °C for 5 min. After brief centrifugation, the supernatants were resolved on a 12% SDS-PAGE. The gel was dried in a gel drier and was exposed to phosphorimaging screen and visualized using phosphorimager.

Expression and purification of his tagged RDR6 using baculovirus system

RDR6 was cloned in the pFASTBacHTA donor vector (Invitrogen, Carlsbad, CA, USA) at EcoRI and SalI sites in the MCS region of the vector. This donor vector provides His tag to the N-terminal of gene of interest. To obtain the recombinant bacmid, DNA isolated from the positive clone was further transformed in to DH10Bac competent *E.coli* cells. DNA was isolated from positive clone for further transfection in Sf21 insect cell line (Invitrogen, Carlsbad, CA, USA). Amplification and titration of the viral stock was done for the large scale expression and purification of RDR6 protein. As per manufacture's instruction recombinant baculovirus stock was transfected to Sf21 cell line. Expression and purification of recombinant RDR6 was confirmed by western blotting using monoclonal anti-His antibody.

RDR6 catalyzed RNA polymerization assay

RDR6 assay was modified from a previous report (Tang et al., 2003). Briefly, assays were conducted at 25 °C in 10 μl reaction mixtures containing 10 mM creatine phosphate, 10 μg/ml creatine kinase, 0.2 unit/μl of RNasin, 500 μM rATP, 100 μM rCTP, 20 μM rUTP, 100 μM rGTP and 5 μCi/ml [α-^{32}P] rUTP, with or without 25–200 ng MBP, GST, MBP-AC2 and GST-AC2$_{\Delta 91-139}$ proteins. 100 ng of 105 nt RNA (without cap and A tail) was used as RDR reaction template. Reactions were initiated by adding final 100 ng of *At*RDR6 purified from Sf21 insect cell line. Reactions were stopped by adding 250 μl TRIzol and 50 μl chloroform. RNA was precipitated by adding 0.6 volume of isopropanol in aqueous phase. RNA pellet was washed with 80% ethanol and air dried for 15 min. RNA was resuspended in 10 μl DEPC treated water followed by adding equal amount of 2 × RNA loading dye. Samples were boiled for 3 min and then placed in ice for 10 min. The samples were resolved on 15% polyacrylamide, 6 M urea gels. The gels were dried and analyzed by phosphorImager. Three independent experiments were performed. The reaction-assay was also carried

out in absence of CTP to differentiate between the RNA-copying and nucleotidyl-transferase activity of RDR6.

Construction of RNAi hairpin loop vector

For the construction of pHANNIBAL-*Nt*RDR6 hairpin loop vector, N-terminal 400 bp of tobacco (*N. tabacum* cv. *Xanthi*) RDR6 (RNA dependent RNA polymerase) sense strand (5′–3′) was cloned into *Xho*I and *Eco*RI sites, while RDR6 (400 bp) antisense (3′–5′) was cloned into *BamH*I and *Xba*I sites of pHANNIBAL vector (CSIRO, Australia). 400 bp of RDR6 gene was amplified from the cDNA of *N. tabacum* cv. *Xanthi* by PCR using Platinum Taq Polymerase. The whole cassette of RDR6 hairpin loop (RDR6 sense–intron–RDR6 antisense) was cloned between CaMV35S promoter and OCS terminator.

Similarly, for the construction of pHANNIBAL-GFP hairpin loop vector, N-terminal 400 bp of GFP sense strand (5′–3′) was cloned into *Xho*I and *Eco*RI sites, while GFP (400 bp) antisense (3′–5′) was cloned into *BamH*I and *Xba*I sites of pHANNIBAL vector. The whole cassette of GFP hairpin loop (GFP sense–intron–GFP antisense) was cloned between CaMV35S promoter and OCS terminator.

Construction of tasiRNA vector

The artificial tasiRNA construct, targeting the AC4 gene of *Tomato leaf curl virus* (ToLCV) (DQ629101), was made using 206 bp AC4 fragment flanked by TAS3 miR390 binding sites. Sequences of miR390 binding sites (5′ binding site for miR390: 5′ggtgctatcctacctgagctt 3′ and 3′ binding site for miR390: 5′cttgtctatccctcctgagcta3′) were derived from putative *Solanum lycopersicum* TAS3 sequence (DV105041). A double stranded 103 bp DNA fragment (*Xho*I–5′miR390 BS–MCS–3′miR390 BS–*Bam*H1) was chemically synthesized (GENEART AG, Germany) and referred as aTAS fragment. aTAS fragment was cloned in pRT100 vector using *Xho*I and *Bam*HI sites. pCAMBIA-2300 (CAMBIA, Canberra, Australia) was used as a final destination vector after removing pUC18 MCS using *Eco*RI and *Sal*I. *Hind*III fallout from recombinant pRT100 vector containing '35S-promoter–aTAS–Nos-terminator' was cloned in pCambia-2300 (pUC18 removed) vector backbone. For cloning AC4, forward primer AC4REPF: 5′-GGGGTACCAGCTGATCGTCCATCGACTT-3′; and reverse primer AC4REPR: 5′-GGAATTCCTCCTCACTTGCATGTGCTC-3′ were synthesized commercially (IDT, USA). The nucleotides underlined represent the restriction sites *Kpn*I and *Eco*RI, respectively, used for cloning. A 206 bp AC4 amplicon was cloned in recombinant binary vector pCambia-2300 at *Kpn*I/*Eco*RI restriction sites in aTAS-MCS. The recombinant clones were named as aTAS-AC4. Plasmid DNA of aTAS-AC4 was mobilized into competent *Agrobacterium tumefaciens* (strain LBA4404). *Agrobacterium* strains with aTAS-AC4, 35S-AC2, 35S-hpRDR6 and pBI empty vector were grown in YEM (0.04% yeast extract, 1% D-mannitol, 0.01% NaCl, 0.02% $MgSO_4$, 0.05% K_2HPO_4; pH 6.8) liquid culture containing kanamycin (50 μg/ml), rifampicin (20 μg/ml) and chloramphenicol (34 μg/ml) at 28 °C, 200 rpm, until the $OD_{600\ nm}$ reached 0.8–1.0. *Agrobacterium* cells were harvested and resuspended in MES buffer [10 mM 2-(N-morpholino) ethane sulfonic acid (MES), 10 mM magnesium chloride ($MgCl_2$)]. Cells were infiltrated into four weeks old tobacco leaves abaxially using a syringe. Small RNA was isolated from infiltrated zones 3 days post infiltration and furthermore tasiRNAs were detected.

In vitro reconstitution of RISC

In vitro reconstitution of RISC assay was modified from a previous report (Baumberger and Baulcombe, 2005). Briefly, *At*AGO1 was overproduced in wheat germ extract using TnT kit. Inflorescences of wild type (WT) *Arabidopsis* plants were ground in liquid nitrogen and protein was extracted in 1 ml/g fresh material of extraction buffer [20 mM Tris–HCl pH 7.5, 4 mM $MgCl_2$, 5 mM DTT and 1tablet/10 ml protease inhibitor (Roche, Basel, Switzerland)]. RISC was reconstituted by mixing overproduced *Arabidopsis* AGO1 (in wheat germ extract) with the WT Col-0 inflorescence extract (1 μg/μl final concentration) in RISC buffer (40 mM HEPES at pH 7.4, 100 mM KOAC, 5 mM $Mg(OAC)_2$, 4 mM DTT). GFP target RNA was *in vitro* transcribed with T7 polymerase in the presence of [α-^{32}P] UTP (3000 Ci/mmol, Perkin-Elmer Life Sciences, USA) and used 50,000 cpm in each reaction. Sixteen microliters of *At*AGO1 overproduced in wheat germ extract coupled with inflorescence extract of *Arabidopsis* was added with 2 μl of specific double strand (ds) $siRNA^{GFP}$ (1 μM) and 0.3 μl of RNasin and incubated for 30 min at room temperature before addition of suppressor or control proteins. Preloaded RISC was further incubated with 2–8 μg of the test suppressors or control proteins for 1 h at room temperature. For controls without any proteins, 1 μl of buffer was added instead. 3.2 μl of substrate cocktail (1 mM ATP, 1 μl α-^{32}P-labeled and capped mRNA, 1.2 μl RNasin) was added to the preloaded RISC in the presence of suppressor or control proteins. The reaction mixtures were incubated for 2 h at 25 °C and RNA was recovered with 250 μl of TRIzol reagent according to the manufacturer's instructions. The labeled RNA was resolved on a 12% urea-polyacrylamide gel and detected after exposure to a PhosphoImager plate.

Sequence of target mRNA:

5′CATCTTCTTCAAGGACGACGGGAACTACAA**GACACGTGCTGAAGTCAAG**TTTGAGGGAGACACCCTCGTCAACAGGATCGAGCTTAAGGGAATCGATTTCAAGGAGG3′

siRNA sequence: 5′ NNGAC ACG UGC UGA AGU CAA G3′

3′CTG TGC ACG ACT TCA GTT CNN 5′

Target site of the siRNA is indicated in bold letter in mRNA sequence.

Acknowledgments

We thank Dr Nirupam Roy Choudhury for technical assistance. We thank Alex Dayton for his critical suggestions during the preparation of the manuscript.

Appendix A. Supplementary material

Supplementary data associated with this article can be found in the online version at http://dx.doi.org/10.1016/j.virol.2015.08.015.

References

Adams, M.J., King, A.M., Carstens, E.B., 2013. Ratification vote on taxonomic proposals to the international committee on taxonomy of viruses. Arch. Virol. 158 (9), 2023–2030.

Agarwal, N., Dasaradhi, P.V.N., Mohammad, A., Malhotra, P., Bhatnagar, R.K., Mukherjee, S.K., 2003. RNA interference: biology, mechanism and application. Microbiol. Mol. Biol. Rev. 67, 657–685.

Akbergenov, R., Si-Ammour, A., Blevins, T., Amin, I., Kutter, C., Vanderschuren, H., Zhang, P., Gruissem, W., Meins Jr., F., Hohn, T., Pooggin, M.M., 2006. Molecular characterization of geminivirus-derived small RNAs in different plant species. Nucleic Acids Res. 34, 462–471.

Allen, E., Xie, Z., Gustafson, A.M., Carrington, J.C., 2005. microRNA-directed phasing during trans-acting siRNA biogenesis in plants. Cell 121 (2), 207–221.

Anandalakshmi, R., Pruss, G.J., Ge, X., Marathe, R., Mallory, A.C., Smith, T.H., Vance, V.B., 1998. A viral suppressor of gene silencing in plants. Proc. Natl. Acad. Sci. USA 95, 13079–13084.

Bartel, D.P., 2004. MicroRNAs: genomics, biogenesis, mechanism, and function. Cell 116 (2), 281–297.

Baumberger, N., Baulcombe, D.C., 2005. Arabidopsis ARGONAUTE1 is an RNA Slicer that selectively recruits microRNAs and short interfering RNAs. Proc. Natl. Acad. Sci. USA 102 (33), 11928–11933.

Baumberger, N., Tsai, C.H., Lie, M., Havecker, E., Baulcombe, D.C., 2007. The Polerovirus silencing suppressor P0 targets ARGONAUTE proteins for degradation. Curr. Biol. 17 (18), 1609–1614.
Bisaro, D.M., 2006. Silencing suppression by geminivirus proteins. Virology 344 (1), 158–168.
Bortolamiol, D., Pazhouhandeh, M., Ziegler-Graff, V., 2008. Viral suppression of RNA silencing by destabilisation of ARGONAUTE 1. Plant Signal Behav. 3 (9), 657–659.
Buchmann, R.C., Asad, S., Wolf, J.N., Mohannath, G., Bisaro, D.M., 2009. Geminivirus AL2 and L2 proteins suppress transcriptional gene silencing and cause genome-wide reductions in cytosine methylation. J. Virol. 83 (10), 5005–5013.
Chapman, E.J., Prokhnevsky, A.I., Gopinath, K., Dolja, V.V., Carrington, J.C., 2004. Viral RNA silencing suppressors inhibit the microRNA pathway at an intermediate step. Genes Dev. 18, 1179–1186.
Chellappan, P., Vanitharani, R., Fauquet, C.M., 2004. Short interfering RNA accumulation correlates with host recovery in DNA virus-infected hosts, and gene silencing targets specific viral sequences. J. Virol. 78, 7465–7477.
Chellappan, P., Vanitharani, R., Fauquet, C.M., 2005. MicroRNA-binding viral protein interferes with Arabidopsis development. Proc. Natl. Acad. Sci. USA 102, 10381–10386.
Curba, J., Chen, X., 2008. Biochemical activities of Arabidopsis RNA-dependent RNA polymerase 6. J. Biol. Chem. 283 (6), 3059–3066.
Di Serio, F., Martinez de Alba, A.E., Navarro, B., Gisel, A., Flores, R., 2010. RNAdependent RNA polymerase 6 delays accumulation and precludes meristem invasion of a viroid that replicates in the nucleus. J. Virol. 84, 2477–2489.
Dong, X., Van Wezel, R., Stanley, J., Hong, Y., 2003. Functional characterization of the nuclear localization signal for a suppressor of posttranscriptional gene silencing. J. Virol. 77 (12), 7026–7033.
Dunoyer, P., Lecellier, C.H., Parizotto, E.A., Himber, C., Voinnet, O., 2004. Probing the microRNA and small interfering RNA pathways with virus-encoded suppressors of RNA silencing. Plant Cell 16, 1235–1250.
Fukunaga, R., Doudna, J.A., 2009. dsRNA with 59 overhangs contributes to endogenous and antiviral RNA silencing pathways in plants. EMBO J. 28, 545–555.
Garcia-Ruiz, H., Takeda, A., Chapman, E.J., Sullivan, C.M., Fahlgren, N., Katherine, J., Brempelis, J., Carrington, C.J., 2010. Arabidopsis RNA-dependent RNA polymerases and dicer-like proteins in antiviral defense and small interfering RNA biogenesis during Turnip mosaic virus infection. Plant Cell 22, 481–496.
Giner, A., Lakatos, L., García-Chapa, M., López-Moya, J.J., Burgyán, J., 2010. Viral protein inhibits RISC activity by argonaute binding through conserved WG/GW motifs. PLoS Pathog. 15 (6), 7.
Glick, E., Zrachya, A., Levy, Y., Mett, A., Gidoni, D., et al., 2008. Interaction with host SGS3 is required for suppression of RNA silencing by tomato yellow leaf curl virus V2 protein. Proc. Natl. Acad. Sci. USA 105, 157–161.
Hao, L., Wang, H., Sunter, G., Bisaro, D.M., 2003. Geminivirus AL2 and L2 proteins interact with and inactivate SNF1 kinase. Plant Cell 15 (4), 1034–1048.
Hartitz, M.D., Sunter, G., Bisaro, D.M., 1999. The tomato golden mosaic virus transactivator (TrAP) is a single-stranded DNA and zinc-binding phosphoprotein with an acidic activation domain. Virology 263 (1), 1–14.
Jeffrey, J.L., Pooma, W., Petty, I.T., 1996. Genetic requirements for local and systemic movement of tomato golden mosaic virus in infected plants. Virology 223 (1), 208–218.
Karjee, S., Islam, M.N., Mukherjee, S.K., 2008. Screening and identification of virus-encoded RNA silencing suppressors. In: Barik, S. (Ed.), 2008. Humana Press, Totowa, NJ, USA, pp. 187–203.
Kasschau, K.D., Carrington, J.C., 1998. A counterdefensive strategy of plant viruses: suppression of posttranscriptional gene silencing. Cell 95, 461–470.
Kasschau, K.D., Xie, Z., Allen, E., Llave, C., Chapman, E.J., Krizan, K.A., Carrington, J.C., 2003. P1/HC-Pro, a viral suppressor of RNA silencing, interferes with Arabidopsis development and miRNA function. Dev. Cell 4, 205–217.
Kim, M.C., Chung, W.S., Yun, D.J., Cho, M.J., 2009. Calcium and calmodulin mediated regulation of gene expression in plants. Mol. Plant 2, 13–21.
Kumar, V., Anand, A., Mukherjee, S.K., Sanan-Mishra, N., 2014. Engineering viral suppressors of RNA silencing: requirement and applications. In: Kumar, A., Lobenstein, G., Reddy, D.V.R. (Eds.), Studium Press Texas, USA.
Kurihara, Y., Watanabe, Y., 2004. Arabidopsis micro-RNA biogenesis through Dicer-like 1 protein functions. Proc. Natl. Acad. Sci. USA 101 (34), 12753–12758.
Lakatos, L., Csorba, T., Pantaleo, V., Chapman, E.J., Carrington, J.C., Liu, Y.P., Dolja, V. V., Calvino, L.F., López-Moya, J.J., Burgyán, J., 2006. Small RNA binding is a common strategy to suppress RNA silencing by several viral suppressors. EMBO J. 25 (12), 2768–2780.
Lecellier, C., Dunoyer, P., Arar, K., LehmannChe, J., Eyquem, S., Himber, C., Saib, A., Voinnet, O., 2005. A cellular microRNA mediates antiviral defense in human cells. Science 308, 557–560.
Li, F., Huang, C., Li, Z., Zhou, X., 2014. Suppression of RNA silencing by a plant DNA virus satellite requires a host calmodulin-like protein to repress RDR6 expression. PLoS Pathog. 10 (2), e1003921. http://dx.doi.org/10.1371/journal.ppat.1003921.
Malik, P.S., Kumar, V., Bagewadi, B., Mukherjee, S.K., 2005. Interaction between coat protein and replication initiation protein of Mung bean yellow mosaic India virus might lead to control of viral DNA replication. Virology 337 (2), 273–283.
Mallory, A.C., Dugas, D.V., Bartel, D.P., Bartel, B., 2004. MicroRNA regulation of NACdomain targets is required for proper formation and separation of adjacent embryonic, vegetative, and floral organs. Curr. Biol. 14, 1035–1046.
Mishra, S.K., Chilikamarthi, U., Deb, J.K., Mukherjee, S.K., 2014. Unfolding of in planta activity of anti-rep ribozyme in presence of a RNA silencing suppressor FEBS letter. FEBS Lett. 588 (10), 1967–1972.
Moissiard, G., Parizotto, E.A., Himber, C., Voinnet, O., 2007. Transitivity in Arabidopsis can be primed, requires the redundant action of the antiviral Dicerlike 4 and Dicer-like 2, and is compromised by viral-encoded suppressor proteins. RNA 13, 1268–1278.
Moissiard, G., Parizotto, E.A., Himber, C., Voinnet, O., 2007. Transitivity in Arabidopsis can be primed, requires the redundant action of the antiviral Dicerlike 4 and Dicer-like 2, and is compromised by viral-encoded suppressor proteins. RNA 13, 1268–1278.
Navarro, L., Dunoyer, P., Jay, F., Arnold, B., Dharmasiri, N., Estelle, M., Voinnet, O., Jones, J.D., 2006. A plant miRNA contributes to antibacterial resistance by repressing auxin signaling. Science 312, 436–439.
Pantaleo, V., Szittya, G., Burgyán, J., 2007. Molecular bases of viral RNA targeting by viral small interfering RNA-programmed RISC. J. Virol. 81 (8), 3797–3806.
Park, W., Li, J., Song, R., Messing, J., Chen, X., 2002. CARPEL FACTORY, a Dicer homolog, and HEN1, a novel protein, act in microRNA metabolism in *Arabidopsis thaliana*. Curr. Biol. 12, 1484–1495.
Pruss, G., Ge, X., Shi, X.M., Carrington, J.C., Vance, V.B., 1997. Plant viral synergism: the potyviral genome encodes a broad range pathogenicity enhancer that transactivates replication of heterologous viruses. Plant Cell 9, 859–868.
Pumplin, N., Voinnet, O., 2013. RNA silencing suppression by plant pathogens: defence, counter-defence and counter-counter-defence. Nat. Rev. Microbiol. 11 (11), 745–760.
Qu, F., 2010. Antiviral role of plant-encoded RNA-dependent RNA polymerases revisited with deep sequencing of small interfering RNAs of virus origin. Mol. Plant Microbe Interact. 23, 1248–1252.
Qu, F., Ye, X., Hou, G., Sato, S., Clemente, T.E., Morris, J.T., 2005. RDR6 has a broad spectrum but temperature-dependent antiviral defense role in *Nicotiana benthamiana*. J. Virol. 79, 15209–15217.
Rahman, J., Karjee, S., Mukherjee, S.K., 2012. MYMIV-AC2, a geminiviral RNAi-suppressor protein, has potential to increase the transgene expression. Appl. Biochem. Biotechnol. 167, 758–775.
Raja, P., Wolf, J.N., Bisaro, D.M., 2010. RNA silencing directed against geminiviruses: post-transcriptional and epigenetic components. Biochim. Biophys. Acta 1799 (3–4), 337–351.
Sanan-Mishra, N., Kuma, V., Sopory, S.K., Mukherjee, S.K., 2009. Cloning and validation of novel miRNA from basmati rice indicates cross talk between abiotic and biotic stresses. Mol. Genet. Genom. 282 (5), 463–474.
Schwach, F., Vaistij, F.E., Jones, L., Baulcombe, D.C., 2005. An RNA-dependent RNA polymerase prevents meristem invasion by Potato virus X and is required for the activity but not the production of a systemic silencing signal. Plant Physiol. 138, 1842–1852.
Siddiqui, S.A., Sarmiento, C., Truve, E., Lehto, H., Lehto, K., 2008. Phenotypes and functional effects caused by various viral RNA silencing suppressors in transgenic *Nicotiana benthamiana* and *N. tabacum*. Mol. Plant-Microbe Interact. 21, 178–187.
Singh, A., Taneja, J., Dasgupta, I., Mukherjee, S.K., 2015. Development of plants resistant to tomato geminiviruses using artificial trans-acting small interfering RNA. Mol. Plant Pathol. 16 (7), 724–734.
Singh, G., Popli, S., Hari, Y., Malhotra, P., Mukherjee, S.K., Bhatnagar, R.K., 2009. Suppression of RNA silencing by Flock house virus B2 protein is mediated through its interaction with the PAZ domain of Dicer. FASEB J. 23 (6), 1845–1857.
Sunter, G., Bisaro, D.M., 1991a. Transactivation of geminivirus AR1 and BR1 gene expression by the viral AL2 gene product occurs at the level of transcription. Plant Cell 4 (10), 1321–1331.
Sunter, G., Bisaro, D.M., 1991b. Transactivation in a geminivirus: AL2 gene product is needed for coat protein expression. Virology 180 (1), 416–419.
Talmor-Neiman, M., Stav, R., Klipcan, L., Buxdorf, K., Baulcombe, D.C., Arazi, T., 2006. Identification of trans-acting siRNAs in moss and an RNA-dependent RNA polymerase required for their biogenesis. Plant J. 48 (4), 511–521.
Tang, G., Reinhart, B.J., Bartel, D.P., Zamore, P.D., 2003. A biochemical framework for RNA silencing in plants. Genes Dev. 17, 49–63.
Tomari, Y., Zamore, P.D., 2005. Perspective: machines for RNAi. Genes Dev. 19 (5), 517–529.
Trinks, D., Rajeswaran, R., Shivaprasad, P.V., Akbergenov, R., Oakeley, E.J., Veluthambi, K., Hohn, T., Pooggin, M.M., 2005. Suppression of silencing by geminivirus nuclear protein AC2 correlates with transactivation of host genes. J. Virol. 7, 2517–2527.
Vaistij, F.E., Jones, L., 2009. Compromised virus-induced gene silencing in RDR6-deficient plants. Plant Physiol. 149, 1399–1407.
Van, W.R., Dong, X., Liu, H., Tien, P., Stanley, J., Hong, Y., 2002. Mutation of three cysteine residues in Tomato yellow leaf curl virus-China C2 protein causes dysfunction in pathogenesis and posttranscriptional gene-silencing suppression. Mol. Plant Microbe Interact. 15 (3), 203–208.
Voinnet, O., 2005. Induction and suppression of RNA silencing: insights from viral infections. Nat. Rev. Genet. 6, 206–220.
Voinnet, O., 2009. Origin, biogenesis, and activity of plant microRNAs. Cell 136, 669–687.
Voinnet, O., Pinto, Y.M., Baulcombe, D.C., 1999. Suppression of gene silencing: a general strategy used by diverse DNA and RNA viruses of plants. Proc. Natl. Acad. Sci. USA 96, 14147–14152.
Wang, H., Hao, L., Shung, C.Y., Sunter, G., Bisaro, D.M., 2003. Adenosine kinase is inactivated by geminivirus AL2 and L2 proteins. Plant Cell 15 (12), 3020–3032.

Wang, H., Buckley, K.J., Yang, X., Buchmann, R.C., Bisaro, D.M., 2005. Adenosine kinase inhibition and suppression of RNA silencing by geminivirus AL2 and L2 proteins. J. Virol. 79, 7410–7418.

Wang, X.B., Jovel, J., Udomporn, P., Wang, Y., Wu, Q., Li, W.X., Gasciolli, V., Vaucheret, H., Ding, S.W., 2011. The 21- nucleotide, but not 22-nucleotide, viral secondary small interfering RNAs direct potent antiviral defense by two cooperative argonautes in *Arabidopsis thaliana*. Plant Cell 23, 1625–1638.

Xie, Z., Qi, X., 2008. Diverse small RNA-directed silencing pathways in plants. Biochim. Biophys. Acta 1779 (11), 720–724.

Xie, Z., Johansen, L.K., Gustafson, A.M., Kasschau, K.D., Lellis, A.D., Ziberman, D., Jacobsen, S.E., Carrington, J.C., 2004. Genetic and functional diversification of small RNA pathways in plants. PLoS Biol. 2 (5), E104.

Zhang, X., Yuan, Y.R., Pei, Y., Lin, S.S., Tuschl, T., Patel, D.J., Chua, N.H., 2006. Cucumber mosaic virus-encoded 2b suppressor inhibits Arabidopsis Argonaute1 cleavage activity to counter plant defense. Genes Dev. 20 (23), 3255–3268.